



Mechanisms of the Early 20th Century Warming in the Arctic

D.D. Bokuchava^{a,b,*}, V.A. Semenov^{a,b}

^a Institute of Geography RAS, Staromonetny per. 29/4, 119017 Moscow, Russia

^b A.M. Obukhov Institute of Atmospheric Physics RAS, Pyzhevsky per., 3, 119017 Moscow, Russia

ARTICLE INFO

Keywords:

Early 20th Century Warming
Global warming
Natural climate variability
Solar irradiance
Volcanism
Anthropogenic aerosols
Black carbon
Greenhouse gases

ABSTRACT

The Early 20th Century Warming (ETCW) in the northern high latitudes was comparable in magnitude to the present-day warming yet occurred at a time when the growth in atmospheric greenhouse gases was rising significantly less than in the last 40 years. The causes of ETCW remain a matter of debate. The key issue is to assess the contribution of internal variability and external natural and human impacts to this climate anomaly. This paper provides an overview of plausible mechanisms related to the early warming period that involve different factors of internal climate variability and external forcing. Based on the vast variety of related studies, it is difficult to attribute ETCW in the Arctic to any of major internal variability mechanisms or external forcings alone. Most likely it was caused by a combined effect of long-term natural climate variations in the North Atlantic and North Pacific with a contribution of the natural radiative forcing related to the reduced volcanic activity and variations of solar activity as well as growing greenhouse gases concentration in the atmosphere due to anthropogenic emissions.

1. Introduction

The rise in global temperatures between 1910 and 1940 is the second strongest warming event during the instrumental global temperature record along with the recent warming. The two warming events are separated by a period of the moderate global temperature decline in 1950s–1970s.

Early 20th century climate fluctuation is of a particular interest nowadays, because it shares some features of the modern warming, despite the fact that greenhouse gas concentrations increase in that time were at least four times smaller compared to the recent decades. The specific features of both episodes are pronounced positive surface air temperature (SAT) anomalies in the Northern Hemisphere (NH), particularly enhanced in high latitudes (e.g., Bekryaev et al., 2010; Xu and Ramanathan, 2012).

The Early 20th Century Warming (ETCW) reached its peak in 1940s (Bengtsson et al., 2004), with maximal 30-year global warming trend of 0.47 °C/30 years in 1916–1945 comparable to the modern warming 30-year trend of 0.56 °C/30 years in 1976–2005 (Fig. 1). Note that the ongoing warming trends have exceeded the maximum rate of warming during ETCW only starting from 1962 to 1991 period. However, all 30-year trends started from 1967 onwards have been constantly stronger (Fig. 1).

The dynamics of temperature changes in the Northern and Southern Hemispheres in the 20th century has significant differences. ETCW has started in the Southern Hemisphere (SH) with the same order anomalies in the beginning of the 20th century and ended up with about 0.18 °C smaller values in the mid-1940s comparing to the temperature evolution in the Northern Hemisphere (Fig. 2). Following the slight insignificant cooling in the 1940s (less than 0.1 °C), the evolution of annual SAT anomalies in the SH shows a monotonous warming since 1960s in contrast to the NH with modern warming commenced in 1975 (Fig. 2). Here, one should be aware of a very sparse data in the SH with a data coverage over land being less than 15% until 1950s that is more than three times smaller than in the NH (Brohan et al., 2006).

In general, slower SH climatic SAT trends in the course of the 20th century in comparison to those in NH can be explained by much larger ocean area in SH with 81% and 61% ocean area in SH and NH respectively that presumably leads to a stronger heat uptake by the ocean and reflects the stronger land surface temperature response to the greenhouse forcing revealed in the climate models simulations (Dommenget, 2009). The different behaviors of the NH and SH long-term SAT anomalies may also indicate different factors of internal variability acting in the two hemispheres and contributing to the climatic trends (Latif et al., 2013).

The distribution of the annual SAT anomalies for various NH

* Corresponding author at: Institute of Geography RAS, Staromonetny per. 29/4, 119017 Moscow, Russia.

E-mail addresses: d.bokuchava@igras.ru (D.D. Bokuchava), vasemenov@ifaran.ru (V.A. Semenov).

latitudinal zones shows that the highest temperature growth for both ETCW and the modern warming periods was observed in the northern polar region (Fig. 3). The difference between the two warming events in NH is expressed in much stronger warming in low latitudes in the recent decades in comparison to the ETCW period, a feature emphasized by Johannessen et al. (2004). The strongest positive annual SAT anomaly in the first half of the 20th century in the Arctic region (60°–90° N) reached 1.8 °C in 1939 relative to 1910 (Fig. 4).

Although the Arctic exhibited the strongest SAT warming in 1940s when considering annual mean zonal temperature anomalies (Fig. 3), high northern latitudes were not the only hotspot during ETCW, especially when looking as summer temperatures. A large part of regional manifestations of the Early 20th Century Warming occurred outside of the Arctic, including across the USA, western Europe, and the north and south Atlantic (Hegerl et al., 2018). There are indications that first record-breaking warm summers in 1930s can be attributed to human influence (King et al., 2016).

The definition of the ETCW period in the Arctic depends on chosen measure and reference period. The temperature increase has started in the end of 1910s with a fast transitions to a warmer (by about 1 °C) climate followed by a more gradual growth with peak values in the end of 1930s and in the 1940s. The cooling starting from the beginning of the 1950s lasted until mid-1960s when it has been reversed by the warming trend (Fig. 4). Here we usually refer to 30 year (1925–1954) period as a core of ETCW anomaly.

ETCW in the Arctic was most pronounced in winter season, while the warming in the 1980s and 1990s was stronger in spring and autumn (Polyakov et al., 2003; Johannessen et al., 2004; Kuzmina et al., 2008) with the temperature increase in winter being relatively moderate.

Winter temperatures in the NH high latitudes during the ongoing warming have reached the anomalies of the 1940s only at the beginning of the 21st century (Semenov, 2007). Furthermore, in some Arctic regions, for example, at the Maliye Karmakuly meteorological station at Novaya Zemlya archipelago (Bulygina et al., 2015) the absolute average annual SAT in 1954 reached –1.4 °C. This at that time was a record-breaking temperature, and was exceeded only in 2012 with –0.9 °C (Fig. 4).

The anthropogenic impact on climate is considered to be the main cause of the modern warming – primarily due to anthropogenic carbon dioxide (CO₂) emissions (Serreze and Francis, 2006). Svante Arrhenius (1859–1927) was the first scientist to suggest (Arrhenius, 1896) that the

fossil fuel burning could lead to a global warming and proposed a relationship between the concentration of carbon dioxide in the atmosphere and surface air temperature. Guy Stewart Callendar in 1938 (Callendar, 1938) confirmed Arrhenius conclusions and suggested that near surface temperature increase over the past 50 years at that time was consistent with the estimated effect of CO₂ concentration growth in the atmosphere due to fuel combustion. This theory was eventually called the “Callendar effect”.

However, the ETCW is comparable by its rate to the modern warming, whereas the growth of CO₂ concentration in the atmosphere in the recent decades is 4–5 time faster than in the middle of the 20th century. This leads to the conclusion that the role of CO₂ could not be as important during ETCW as for the modern warming. Furthermore, the monotonous CO₂ concentration increase was also inconsistent with the global SAT decline from the 1950s to the 1970s.

A comprehensive theory explaining ETCW and its stronger manifestation in high latitudes is still a matter of debate. Climate models point to the important role of internal natural climate variability (Delworth and Knutson, 2000) and positive feedbacks enhancing climate variations in high latitudes (Bengtsson et al., 2004; Chen et al., 2018), external natural factors (Nozawa et al., 2005; Suo et al., 2013), external anthropogenic factors, including sulphate and soot aerosols (Shindell and Faluvegi, 2009; Booth et al., 2012) and greenhouse gases (GHG) (Meehl et al., 2004) as potential drivers of this climate anomaly.

Numerical experiments with different generations of climate models ensembles (IPCC, 2001, 2007, 2013) show that more accurate and realistic consideration of different external factors impacting climate (natural and anthropogenic) leads to in general a better reproduction of SAT changes on global and regional scales over the past 150 years, including ETCW. However, while the modern warming is almost perfectly reproduced when averaged over the model ensembles (indicating external influence as the major factor), the ETCW amplitude, despite the increasing accuracy of model simulations, still remains significantly underestimated in climate models when compared to the observations. Ensemble mean Arctic SAT variations as simulated in CMIP3, 5 and 6 ensembles under historical external anthropogenic and natural forcing in comparison to observational data are shown in Fig. 5a. Apart from the apparently underestimated ETCW magnitude, the models do show some cooling in 1960s preceded by the warming, the latter peaks later than the observed (in 1950s). One may also note that the magnitude of the ETCW in CMIP5 and 6 ensembles (measured as a

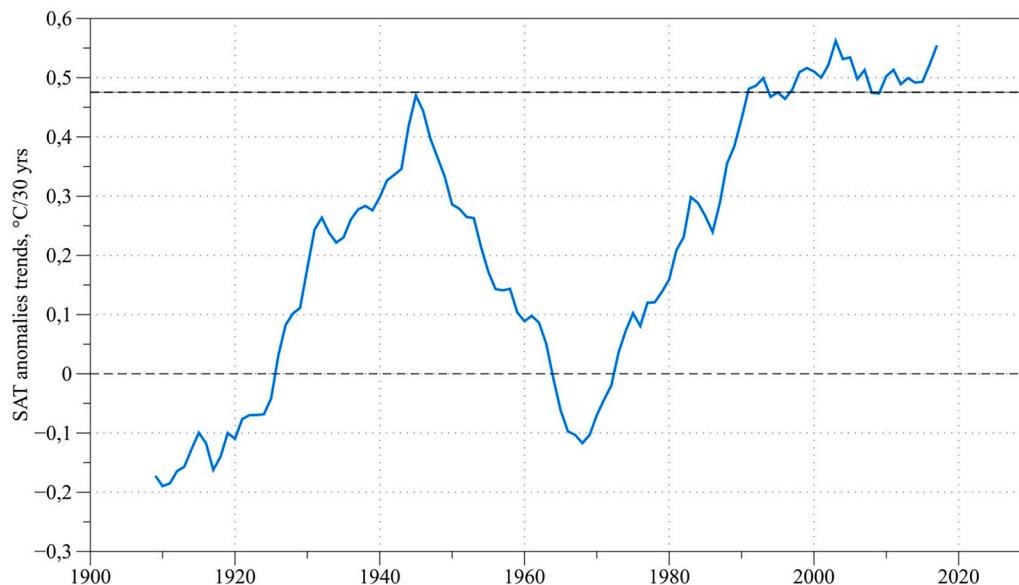


Fig. 1. 30-year moving trends of global annual mean SAT anomalies (°C/30 years) according to Berkley dataset (Rohde, 2013). The year corresponds to the end of the 30-yr moving window.

temperature difference between peak values in 1950s and low values in 1910s) is roughly as twice as larger than in CMIP3 ensemble.

The disagreement between the observed and simulated (in response to external forcing) Arctic SAT indicates the important role of internal climate variation on multi-decadal time scale (Delworth and Knutson, 2000; Bengtsson et al., 2004; Latonin et al., 2021). Climate models are capable to produce large internal variations that are similar to the observed. This is illustrated in Fig. 5b where some examples of such single-run model realizations are presented.

It is also important to note that we should not exclude a possibility of incorrectly specified external natural and anthropogenic aerosol forcing in the first half of the 20th century, when the uncertainty of data is much higher than for the period of the ongoing warming.

The majority of studies (e.g., Delworth and Knutson, 2000; Suo et al., 2013; Hegerl et al., 2018) agree that such a strong warming anomaly as ETCW can be explained by a combination of internal climate system variability manifested as quasi-periodic oscillations or a random climate fluctuation with increasing global temperature at the background caused by external anthropogenic and natural forcing (increased GHG emissions and a pause in volcanic eruptions, in particular).

Analysis of ETCW is complicated by insufficient quantity and quality of observational data. Our knowledge about surface air temperature variations during that period is based on irregular meteorological station observations on land, measurements from ships, and some climate reconstructions (e.g., Hansen et al., 2010). The spatial data coverage during the early warming is characterized by large gaps in key regions covered only by sporadic measurements, for example, in the tropical Pacific and most of the Southern Hemisphere, in central Africa, and in polar latitudes (Morice et al., 2012; Rohde, 2013; Hegerl et al., 2018). Data scarcity is a particular problem for Polar Regions, where the majority of about 200 meteorological land stations during ETCW period represented European/Scandinavian sector with large gaps in northern Siberia and North America (Bekryaev et al., 2010). The vast area of Arctic Ocean has not been and is still not covered by in situ observations. Knowledge about historical temperature variations over multiyear sea ice used to come from manned drifting stations or irregular expeditions (Kuzmina et al., 2008). In this study, Berkeley Earth temperature data set (Rohde, 2013; <http://berkeleyearth.org/>) is often used for illustrations. These data comprise the maximal number of available observational records, are based on state of the art reconstruction techniques to

provide a global coverage, and are claimed to show a better accuracy (Rohde, 2013). In fact, all three major modern global SAT empirical data analyses (GISS Surface Temperature Analysis (Lenssen et al., 2019; <https://data.giss.nasa.gov/gistemp/>), HadCRUT (Morice et al., 2021) using land temperature CRUTEM5 (<https://crudata.uea.ac.uk/cru/data/temperature/>) and Berkeley Earth data) exhibit very similar temperature variations in the Arctic. Fig. 6a shows annual mean SAT anomalies over land north to 60° N based on three aforementioned dataset with and without masking NASA and Berkeley Earth data according to CRUTEM5 data coverage (that is the least among the datasets). No noticeable differences between data sets can be seen after 1920, particularly after applying the same missing value mask. Before 1920, Berkeley Earth data show systematically warmer anomalies with the discrepancy reduced after applying masking procedure.

An alternative data source is atmospheric reanalyses (Lindsay et al., 2014) that cover the entire 20th century and provide a complete set of meteorological data with 100% spatial coverage. It is tempting to use 20th century reanalyses for climate and weather studies in the ETCW period in the same way as the currently updated reanalyses (e.g., NCEP/NCAR, ERA, JRA-55, MERRA2, see, e.g. Rohrer et al. (2018) for inter-comparison and references) are used for the period since 1950s or later onwards. This, however, should be done with caution.

A reanalysis is a result of numerical experiments with atmospheric or coupled atmosphere-ocean model that assimilate available observational data and pull atmospheric (and ocean) dynamic and thermodynamic variables toward the available observations by using additional relaxation term in evolution equations. In case of the 20th century reanalyses, due to the lack of other long-term data, sea level pressure (SLP) is the only atmospheric variable used for the assimilation. SLP data are also highly limited in the early 20th century period in vast areas around the globe and fully missing over the Arctic Ocean (even nowadays). This so called “fog of ignorance” in assimilated data makes vague a picture of reanalyzed climate variations in the first half of the 20th century. Furthermore, reanalysis models employ empirical data on sea surface temperatures (SST) and sea ice concentrations (SIC) as lower boundary conditions. The latter are particular uncertain in the Arctic in the first half of the century. Commonly used SST/SIC HadISST versions 1 and 2 datasets (also used as boundary conditions in reanalysis products) exhibit no large decadal to interdecadal Arctic Sea ice extent variations before 1950s, whereas new reconstructions reveal a strong negative sea

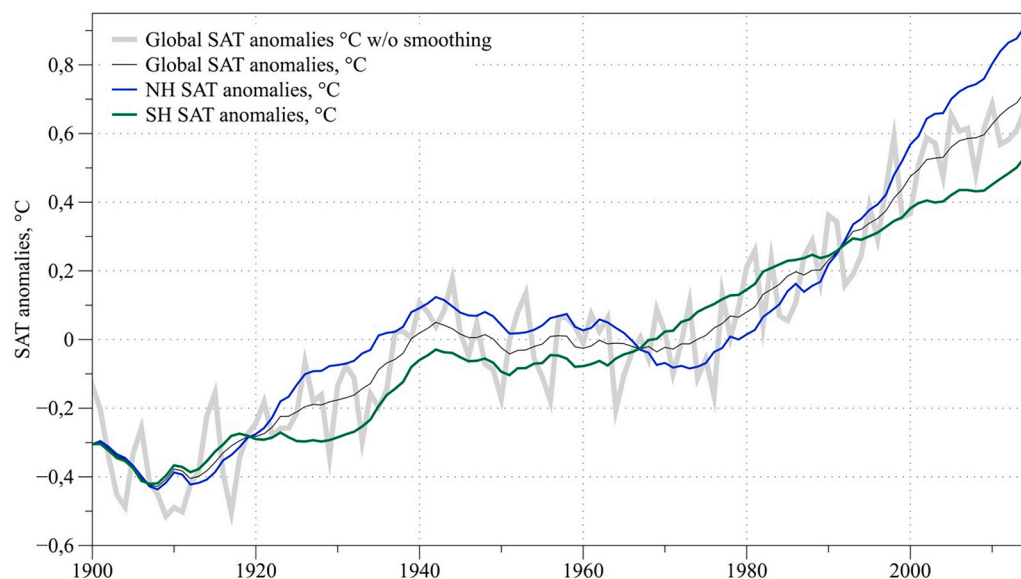


Fig. 2. Average annual SAT anomalies (°C) – Global (black curve), NH (blue curve), SH (green curve) and Global without running mean smoothing (gray curve), according to Berkeley dataset. The reference period for temperature anomalies is 1951–1980, 11-year running mean (For interpretation of the references to colour in this figure legend, the reader is referred to the web version of this article.)

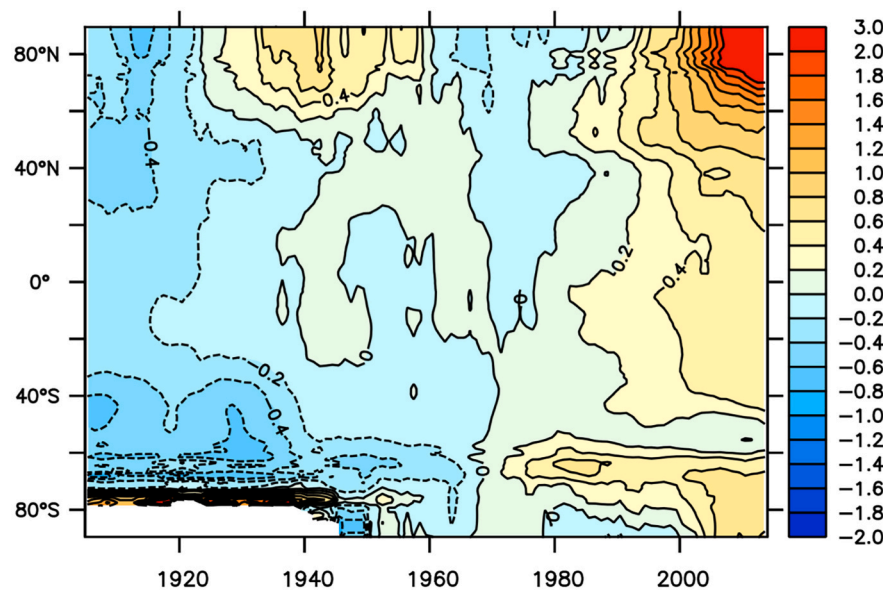


Fig. 3. Zonally averaged annual SAT anomalies (°C) according to Berkley dataset. The reference period for temperature anomalies is 1951–1980, 11-year running mean

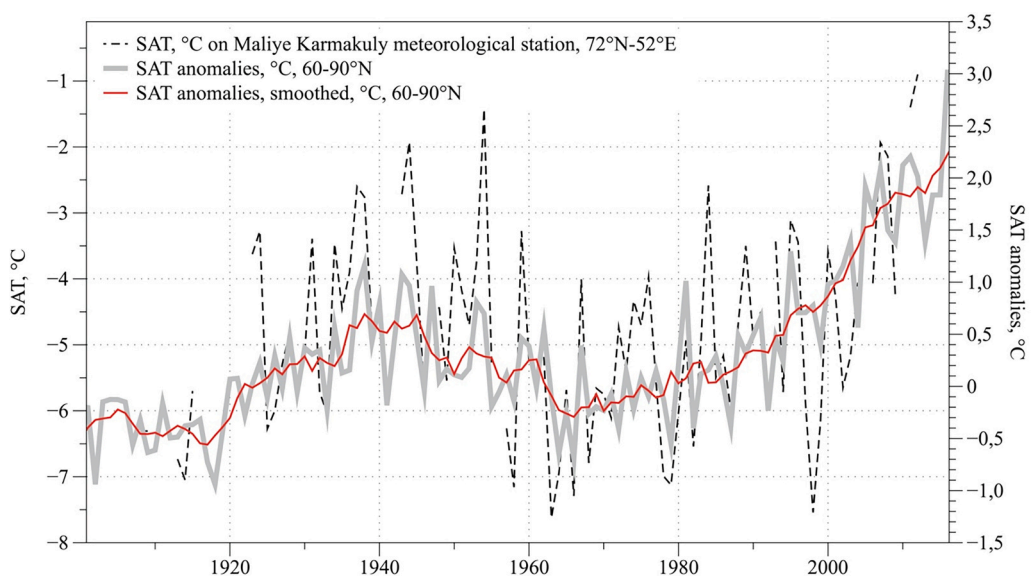


Fig. 4. The average annual SAT, °C at the polar meteorological station “Maliye Karmakuly” located at south-western part of Novaya Zemlya (72°22′24″N, 52°43′00″E) (black dotted curve); average annual SAT anomalies, °C, with 5-year running mean smoothing (red line) and without smoothing (gray line) for the Arctic region (60–90°N), according to Berkley dataset. The reference period for temperature anomalies is 1951–1980. (For interpretation of the references to colour in this figure legend, the reader is referred to the web version of this article.)

ice anomaly concurrent with ETCW (Walsh et al., 2017; Semenov and Matveeva, 2020; Brennan et al., 2020). An atmospheric general circulation model when forced with prescribed SIC data without negative sea ice anomaly in the Arctic during ETCW period could not reproduce the concurrent Arctic temperature anomaly (Semenov and Latif, 2012). This also suggests a crucial role of the highly uncertain sea ice data for correct representation of the Arctic climate during ETCW period in reanalyses. It is illustrated in Fig. 6b, where Arctic SATs from three 20th century reanalyses are compared with each other and observations. Two atmosphere reanalyses, NOAA20C (Compo et al., 2011) and ERA20C (Poli et al., 2016), and one coupled reanalysis, CERA20C (Laloyaux et al., 2018) are used. The comparison reveals significant Arctic temperature variations in the first half of the century in all reanalyses, that indicates that these data should not be used as a replacement for missing observations in aforementioned period (Bokuchava and Semenov, 2018).

Understanding the nature of ETCW is a key to determine the relative contribution of internal variability and external natural and

anthropogenic forcings to the global and regional climate variations (Brönnimann, 2009). Analysis of SAT changes in high latitudes during the first half of the 20th century allows us to identify possible mechanisms of natural and externally forced climate variability and positive feedbacks in the Arctic climate system fostering enhanced climate variations (Pithan and Mauritsen, 2014; Semenov, 2015).

This paper provides an overview of the existing hypotheses that may explain ETCW, describes the main mechanisms of internal and external climate variability during the 20th century, focusing on the Arctic region. The article is organized as follows: Section 2 describes processes responsible for the amplified climate variations in the Arctic, Sections 3 and 4 consider natural internal and external factors respectively, and Section 5 deals with the anthropogenic impacts in the early 20th century period.

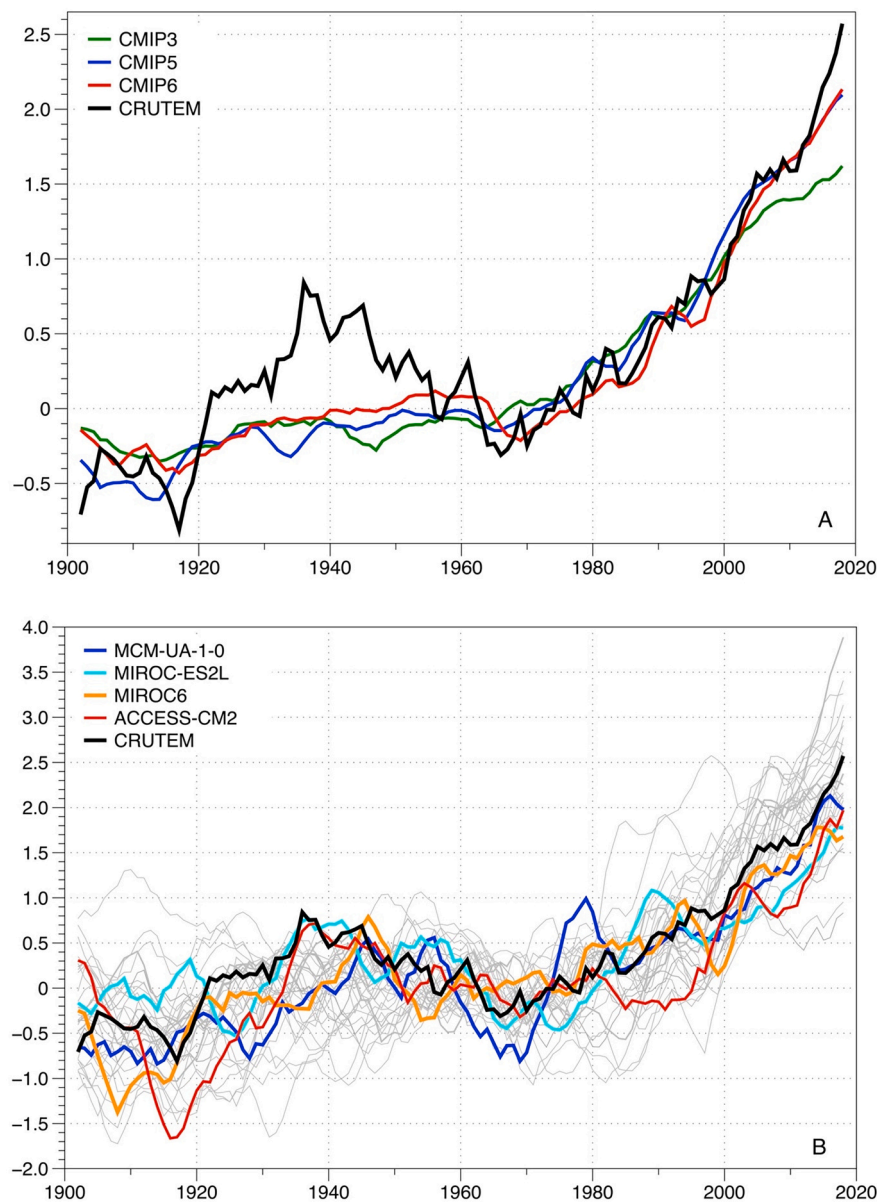


Fig. 5. Annual Arctic SAT anomalies ($^{\circ}\text{C}$ as observed (CRUTEM5 data) and (a) averaged (ensemble mean) over CMIP3, 5 and 6 model simulation ensembles (a); and as simulated in individual models from CMIP6 ensemble (gra lines) with highlighted (by thick colored lines) simulations that exhibit multidecadal SAT variations similar to ETCW (b). All data are masked as in CRUTEM5 data set. The reference period for temperature anomalies is 1951–1980, 5-year running mean

2. Amplified climate variations in the Arctic

A specific feature of ETCW in the Arctic is its higher amplitude in comparison to the global or hemispheric changes (Fig. 2). The rate of temperature increase in the Arctic region in the first half of the 20th century was approximately three times higher than the warming in the Northern Hemisphere on average (Bekryaev et al., 2010). The same feature is evident for the modern warming as well. The larger temperature increase near the poles compared to the global mean changes is often referred as to “Polar (or Arctic) Amplification” (AA). Such variability feature is related to different positive radiation and dynamical/thermodynamical feedbacks as well as to a contribution from internal climate variability modes. The positive feedbacks may enhance and sustain an initial climate fluctuation caused by internal variability or external forcing and thus explain ETCW in the Arctic (e.g., Bengtsson et al., 2004). Here, some important positive feedbacks that may have contributed to ETCW are overviewed.

Positive radiation feedbacks include a surface albedo–temperature

feedback that can enhance amplitude of climate variations. A general idea of that reduction of snow and ice cover with growing temperature leads to higher solar radiation absorption and further warming was formalized in the first energy balance models (Budyko, 1969). Until recently this feedback has been considered as the major factor leading to AA (Winton, 2006).

The Arctic Amplification is also simulated in climate model experiments without albedo–temperature feedback (Hall, 2004; Graversen and Wang, 2009) and may be caused by other positive feedbacks (Pithan and Mauritsen, 2014). For example, intensified ice melting results in an increase of water vapor content and cloud cover, which lead to a stronger greenhouse effect more pronounced in high latitudes (Graversen and Wang, 2009). Arctic Amplification may also result from large scale thermodynamical mechanisms such as enhanced northward latent heat transport in the warmer atmosphere despite the reduced equator–pole temperature gradient and weaker meridional circulation (Alexeev et al., 2005; Caballero and Langen, 2005).

ETCW can also be associated with positive dynamical feedbacks,

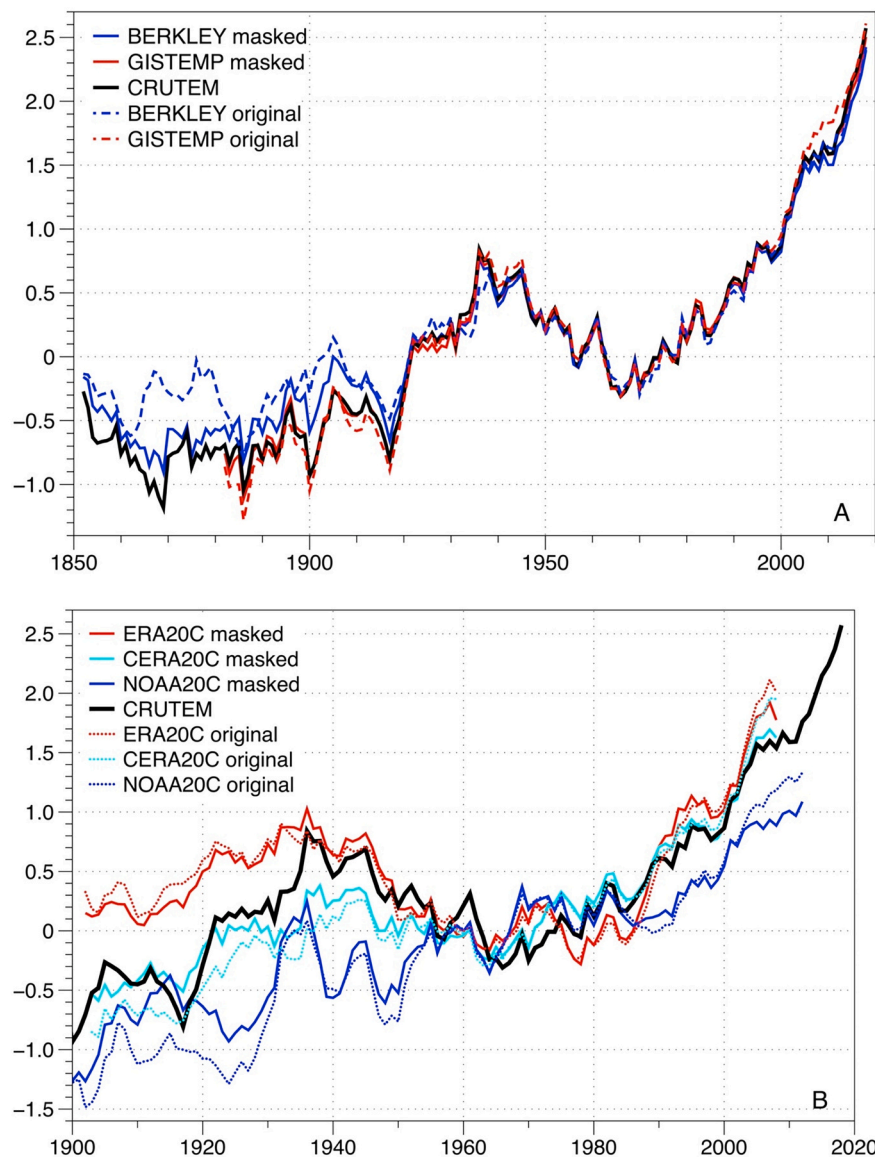


Fig. 6. Arctic annual mean SAT anomalies, ($^{\circ}\text{C}$) over land area north of 60°N (a) from GISS, CRUTEM5 and Berkely Earth data sets in original form (dashed lines) and when masked according to CRUTEM5 missing data (solid lines), see the legend, and (b) from NOAA20C, ERA20C and CERA20C reanalysis products, also original and CRUTEM5-masked (dashed and solid accordingly, see the legend). The reference period for temperature anomalies is 1951–1980, 5-year running mean.

which enhance initial temperature changes by dynamical processes modulating oceanic and atmospheric heat transport to the Arctic. For example, sea ice reduction in the Barents Sea leads to a cyclonic atmosphere circulation response that enhances oceanic inflow of warm Atlantic waters to the Sea with further sea ice retreat. Such a mechanism was proposed as a possible explanation for ETCW in the Arctic (Bengtsson et al., 2004). There are other dynamical positive feedbacks suggested to contribute to the accelerated modern warming in the Arctic that might have also contributed to ETCW event. They include a positive feedback between sea ice thickness and heat exchange between Atlantic water and ocean surface (Ivanov et al., 2016, 2018), and sea ice cover and water vapor (Alexeev et al., 2017). These feedbacks operate in the Atlantic Sector of the Arctic and imply a role of varying oceanic heat transport as an important factor for ETCW.

Quasi-periodic fluctuations of North Atlantic sea surface temperature (SST) on 60–80 year time scale (Schlesinger and Ramankutty, 1994) usually referred to as Atlantic Multidecadal Oscillation (AMO) are related to oceanic heat transport in the Barents Sea throughout the 20th century (Levitus et al., 2009) and could be a source of initial climate

variations further enhanced by the aforementioned positive feedbacks.

Changes in the Arctic climate system can lead to significant changes in atmosphere circulation and temperature conditions in the northern mid-latitudes. The heating of the lower troposphere over the Barents-Kara Seas in winter due to sea ice reduction may result in occurrence of atmospheric blocking in, and south of, the Barents Sea region (Petoukhov and Semenov, 2010; Semenov and Latif, 2015). This causes an enhanced anomalous advection of cold Arctic air to the NH continents that leads to more frequent anomalously cold winters in the beginning of the 21st century in the Northern Eurasia and North America (Petoukhov and Semenov, 2010; Kug et al., 2015). This overall cooling in mid-latitudes related to weakening of the zonal flow in response to sea ice retreat and warming in the Arctic could lead to a stronger AA.

The winter SAT pattern of contrasting strongly positive temperature anomalies centered over the Barents Sea and negative anomalies over Siberia (Fig. 7) have recently received a lot of attention. The pattern was called – “Warm Arctic-Cold Siberia” (Warm Arctic – Cold Siberia – WACS) or Warm Arctic-Cold Continent (Warm Arctic – Cold Continent –

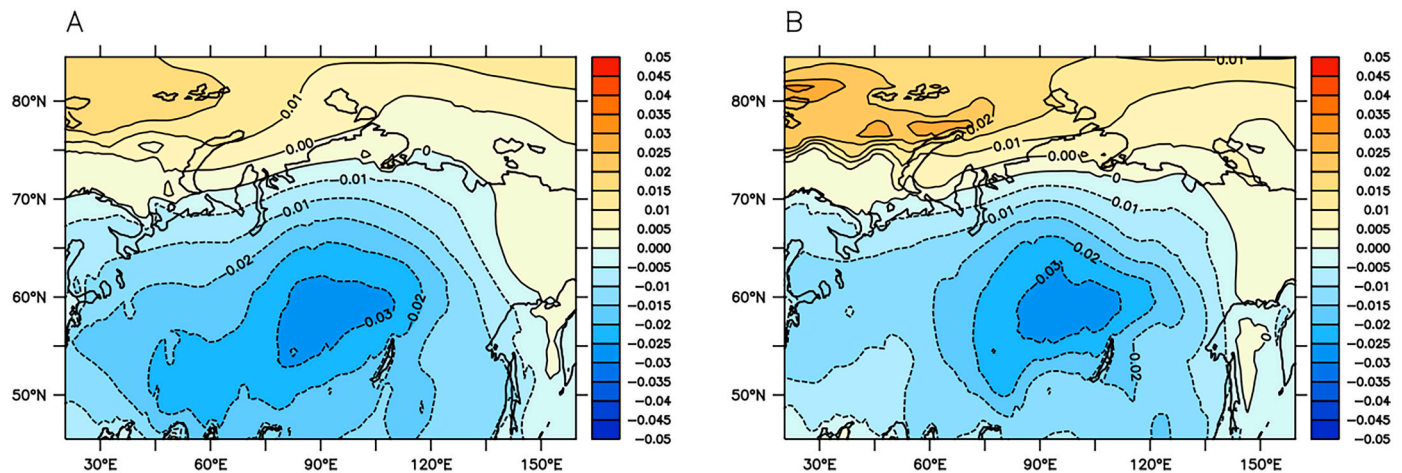


Fig. 7. WACS pattern (winter (DJF) EOF-2 SAT in 20–100° E, 45–80° N region, for two warming periods 1925–1954 (A) and 1981–2020 (B), according to Berkley dataset. The reference period for temperature anomalies is 1951–1980.

WACC) and is observed not only in the current period of Arctic warming, but also during ETCW (Wegmann et al., 2018; Chen et al., 2018). A similarity of the regional temperature variability patterns that are related to a specific circulation response during ETCW and the modern warming suggest a role of similar feedback and response processes during the both warming periods.

3. Natural internal factors

3.1. Atmosphere circulation variability

The major problem of disentangling climate change mechanisms is related to quantifying relative contributions of internal natural variability and external anthropogenic and natural forcing (Delworth and Knutson, 2000). Noticeable temperature trends in the 1920s and 1940s had already been a subject of scientific interest in the first half of the 20th century (Kincer, 1933). Some studies have showed the important role of atmospheric and oceanic circulation in regional climate changes (e.g., Vise, 1937). The analysis of the Arctic climate variability in the 20th century reveals long-term quasi-cyclic changes of different frequencies associated with coupled atmosphere-ocean dynamics in the North Atlantic and the Arctic (Proshutinsky and Johnson, 1997; Frolov et al., 2006).

Numerical experiments with CMIP3 climate models (Wang et al., 2007) show that internal climate variability can result in the Arctic temperature fluctuations of comparable to ETCW amplitude but on decadal time scale, while the observed mid-20th century event was interdecadal. Recent analysis reveals that about a half of the global warming in the first part of the 20th century is a result of a combination of natural intrinsic variability and anthropogenic forcing (Hegerl et al., 2018). A significant part of interannual and long-term SAT variance in the Arctic can be explained by variations of major atmospheric circulation patterns (Wood and Overland, 2010). The key regions responsible for the air masses inflow to the Arctic are the North Atlantic and the North Pacific Ocean sectors. In the second half of the 20th century, leading atmosphere variability modes such as the North Atlantic Oscillation (NAO), the Arctic Oscillation (AO) and the Pacific North American (PNA) Oscillation together explained 44% of the Arctic SAT variance (Wood and Overland, 2010), whereas the NAO alone could account for around 45% of the winter warming in the Northern Extratropics in the late 20th century (Iles and Hegerl, 2017). These variability modes could also be an important driver of ETCW.

The AO or Northern Annular Mode (NAM) and related NAO are the dominant modes of large-scale winter atmospheric variability in the Northern Hemisphere Extratropics. The AO is usually defined as the first

EOF of the winter sea level pressure (SLP) field in the Northern Hemisphere and consists of dipole in SLP between the North Atlantic/Pacific Oceans and the Arctic (Ambaum et al., 2001). The NAO is the leading SLP variability mode in the North Atlantic/European Sector and characterized by SLP dipole with one center over Greenland (Icelandic minimum) and another center one in the North Atlantic mid latitudes (Azores maximum) (Stephenson et al., 2003). The NAO is often considered as a regional manifestation of the AO. The AO in general reflects a strength of the polar vortex, whereas the NAO characterizes the intensity of westerly flow over the northern North Atlantic and Europe, and the position of storm tracks in the North Atlantic sector. This largely determines the winter climate in the northern North Atlantic, Northern Eurasia and the Arctic (Ambaum et al., 2001; Moritz et al., 2002).

During the first three decades of the 20th century, the positive phase of the NAO (Fig. 8) reflected a stronger than usual zonal winds over the northern North Atlantic. The long-term dominance of this atmospheric circulation pattern led to the advection of heat to the northeastern part of the North Atlantic and to the Atlantic sector of the Arctic. However, the NAO transition to a negative phase after 1930 and the inconsistency between the NAO and Arctic SAT variations before 1950 (Fig. 8) do not support a hypothesis of NAO contribution to the ETCW warming (Semenov and Bengtsson, 2003). It is suggested that NAO reduced the winter warming in the NH by more than 50% during 1920–1971 period (Iles and Hegerl, 2017). Furthermore, a link between the NAO and Arctic SAT variability was found to be strongly non-stationary varying from statistically significant positive correlations to negative correlation in different multi-decadal periods (Semenov, 2007; Smedsrud et al., 2013).

The NAO was also suggested to be impacted by the Arctic Sea ice loss through different hypothesized mechanisms (e.g., Cohen et al., 2014; Mokhov and Semenov, 2016). As we now know, the rapid sea ice loss may explain the negative NAO trend since mid-1990s. Given that ETCW was accompanied by the Arctic Sea ice area decline (see earlier discussion), one may hypothesize that the decrease of the NAO index in 1920s–1930s could be influenced by the concurrent sea ice changes. It is important to note that the link between sea ice loss and circulations response can be non-linear as was first suggested by Petoukhov and Semenov (2010), and further elaborated in Semenov and Latif (2015), Overland et al. (2016). The emergence of WACS pattern and circulation response to sea ice changes may in turn also depend on the NAO phase (Luo et al., 2016).

The Pacific North American Oscillation index (PNA) characterizes the pressure gradient between the northern North Pacific (Aleutian minimum) and the north-eastern part of North America (Canadian maximum). This gradient is related to a strength of North Pacific zonal

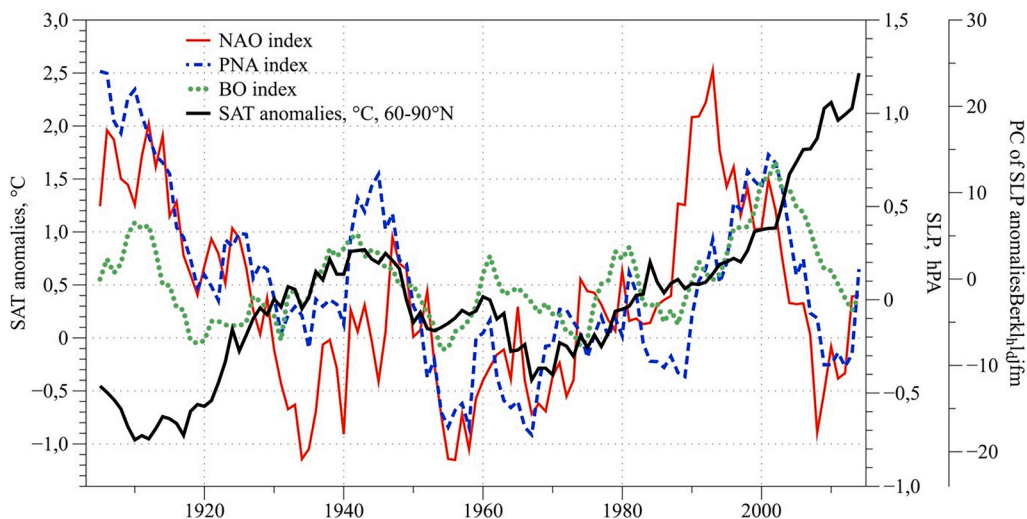


Fig. 8. Winter (DJFM) Arctic (60–90°N) SAT anomalies(°C) for 1900–2015 (black curve) according to Berkeley dataset, the reference period for temperature anomalies is 1951–1980, 7-year running mean. NAO index defined as a DJFM sea level pressure difference between Iceland minimum and Azore maximum (red curve), PNA index defined as the first principal component (PC) of winter SLP variability over 30–90°N region (blue curve) and Barents Oscillation index as the second PC of winter SLP variability over 60–90°N, 90–180°E region (green curve). SLP data are from HadSLP2.0 dataset (Allan and Ansell, 2006). (For interpretation of the references to colour in this figure legend, the reader is referred to the web version of this article.)

flow. An important feature of PNA in the context of ETCW is that both (positive and negative) PNA phases may contribute to atmospheric heat advection to the Arctic in different regions. As stated by Hegerl et al. (2018), atmospheric circulation related to a negative PNA pattern in 1930s allowed poleward transport of warm air masses over the northwestern Pacific (Wegmann et al., 2017). A strong positive peak in the PNA then followed in the early 1940s (Fig. 8), which brought warm air toward western Canada and into Alaska, followed by an abrupt drop in the 1950s. Both these circulation anomalies contributed to Arctic warming. PNA is strongly influenced by the El Niño/Southern Oscillation (ENSO), with positive indices usually associated with El Niño phenomena, and negative indices related to La Niña events (Philander, 1990). In particular, the weak PNA in 1930s could be related to the lack of ENSO activity in the 1930s (e.g., Schubert et al., 2004).

It is also important to emphasize regional atmospheric variability patterns defined in geopotential height anomalies or SLP in the North Atlantic and North Pacific Oceans: Eurasia – East Atlantic, East Atlantic – Western Russia, Scandinavian patterns (Barnston and Livezey, 1987), and Barents Oscillation (Tremblay, 2001; Chen et al., 2013) associated with atmospheric heat transport to the high latitudes. They may significantly impact Arctic climate on a time scale from interannual to decadal. Such regional atmospheric variability may contribute to the Arctic SAT anomalies on a regional scale.

Analysis of tropospheric circulation shows that the internal atmosphere dynamics may have had an impact on the Arctic SAT in the first half of the 20th century. Contributions of both the Atlantic and Pacific Sectors to the transport of warm maritime air masses into the Arctic were suggested (Wegmann et al., 2017). This, however, cannot explain the entire amplitude of ETCW (Hegerl et al., 2018) and should be complemented by other factors of external or internal variability.

3.2. Ocean circulation variability

Arctic Amplification in the 20th century including the modern warming and ETCW periods can be associated not only with a number of positive feedbacks inherent in the Arctic climate system or with an increase of atmospheric heat transport, but may also result from an enhancement of oceanic heat inflow from the North Atlantic to the Arctic (Delworth and Mann, 2000; Polyakov et al., 2004; Levitus et al., 2009; Semenov et al., 2014). The heat transported from low to high latitudes of the Atlantic ocean is basically released to the atmosphere in the Atlantic sector of the Arctic. A positive anomaly of the heat transport causes an enhanced Arctic warming and may significantly impact hemispheric and global temperatures, in particular explaining up to 50% of the warming in the Northern Hemisphere in the last three decades of

the 20th century (Semenov et al., 2010).

An analysis of climate model simulations shows that ETCW in the Arctic may be a result of increased oceanic inflow from the North Atlantic to the Barents Sea with a corresponding retreat of the sea ice (Bengtsson et al., 2004), and also points to a link between inter-decadal temperature variability in the Arctic and quasi-periodic oscillations of thermohaline circulation in the North Atlantic (Delworth and Mann, 2000). Thermohaline circulation also often referred to as the ocean conveyor is driven by large-scale temperature and salinity gradients that determine a density of sea water. It is largely responsible for the heat transport between ocean basins (Lappo et al., 1990) and, in particular for the northward ocean heat transport in the North Atlantic (Delworth and Mann, 2000). Quasi-periodic variations of this heat transport may lead to global climate anomalies and, in particular, contribute to the modern warming (Semenov et al., 2010).

Instrumental data show that SST variability in the North Atlantic during the 20th century was dominated by quasi-cyclic variability on a 50–80 year timescale, usually referred to as the AMO. During the instrumental record, there are two distinct warm periods in the 1930s–1940s and since 1980s, and two cold periods in the beginning of the 20th century and in the 1960s–1970s (e.g., Polyakov et al., 2004). The observational data also indicate AMO-like cycles in the observed multidecadal variations of the Arctic SAT from the beginning of the 20th century are concurrent with AMO cycles (Fig. 9).

Paleo-reconstructions of AMO demonstrate that strong low-frequency (60–100 years) SST variability is a robust feature of the North Atlantic climate over at least the past five centuries (Gray et al., 2004). There are also indications of a significant correlation between Arctic Sea ice area and AMO in the last centuries including ETCW period (Miles et al., 2014). Time series of the 100–150 m depth layer temperature in the Barents Sea during the 20th century reveals multidecadal variability, which is consistent with long-term AMO variations (Levitus et al., 2009). These all make AMO the major candidate for the natural variability factor contributing to ETCW.

The link between atmospheric circulation in the Northern Pacific and the Arctic climate variations brought about new hypotheses for ETCW that involve regional oceanic variability factors (Hegerl et al., 2018). The most plausible ones involve the Pacific Decadal Oscillation (PDO), which reflects a decadal to inter-decadal variability of the Pacific SSTs north of 20° N and has a 20–40 years quasi-periodicity (Mantua et al., 1997). It could have played at least an equally important role in the heat advection to the Arctic in the middle of the 20th century (Wegmann et al., 2017) or even become a major factor in the formation of ETCW (Svendsen et al., 2018).

Several recent studies (Tokinaga et al., 2017; Wegmann et al., 2017;

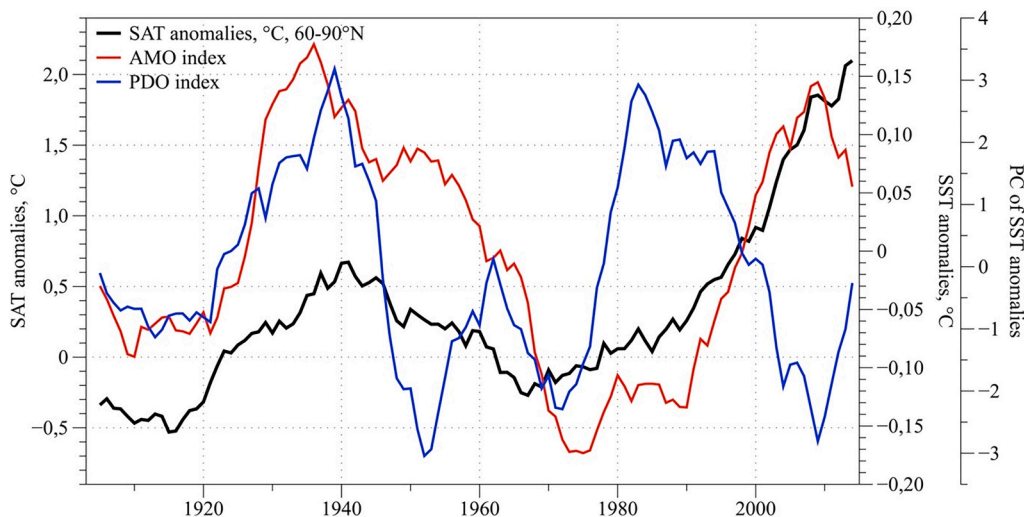


Fig. 9. Annual Arctic (60–90°N) SAT anomalies, (°C) for 1900–2010 (black curve) according to Berkeley dataset, the reference period for temperature anomalies is 1951–1980, 7-year running mean. AMO index as averaged annual detrended SST anomalies, °C, over 0–60°N, 80°W–8°E region (10-year running mean, red curve), PDO index as the first PC of the averaged annual detrended SST anomalies, °C, over 20–60°N, 120–240°E region (10-year running mean, blue curve) according to HadiSST2.0 dataset (Titchner and Rayner, 2014). (For interpretation of the references to colour in this figure legend, the reader is referred to the web version of this article.)

Malinin and Vainovsky, 2018) analyzing both observational data and model experiments, suggested that the synchronous phase shift of the AMO and PDO has largely contributed to the accelerated Arctic warmings in the 20th century, both the ongoing one and ETCW.

The issue of relative roles of the PDO and AMO in the Arctic warming remains controversial. An analysis of CMIP5 ensemble simulations (Chylek et al., 2016a, 2016b) show that PDO (unlike AMO) is not a statistically significant predictor for the global SAT changes in the 20th century, while Steinman et al. (2015) find that both AMO and PMO are able to explain a large proportion of internal variability in NH mean temperatures. Other studies, e.g. by Svendsen et al. (2018) using coupled climate model experiments argue that PDO alone could be a key factor in the Arctic warming during ETCW. Their numerical simulations show that the shift of PDO to a positive phase in 1920s resulted to a deeper Aleutian low and enhanced advection of warm air masses to the Arctic in the Pacific sector. Furthermore, they find that the changes in Pacific SSTs in that time could have weakened the polar vortex leading to air descent and adiabatic heating of the lower troposphere in the Arctic. The important role of PDO is supported by Kosaka and Xie (2016) who identify, using global atmosphere-ocean coupled model, the tropical part of the Pacific Ocean as a key region for long-term global climate variations in the last century, particularly in the 1910s–1940s. The uncertainty with the assessment of the PDO role is in general related to the fact that the results are based on dedicated atmospheric or coupled model simulations and thus depend on a model and a simulations setup. On top of that some studies suggest that state-of-the-art climate models in general fail to reproduce features (magnitude, spatial patterns and their sequential time development) of the observed multidecadal variability correctly (Kravtsov et al., 2018).

The difference between the PDO and AMO influence may be related to their different dominant variability time scales. PDO variations are expressed on both decadal and multidecadal time scales (McCabe et al., 2004) (Fig. 9), while changes in the Atlantic SSTs are characterized by dominant 60–70-year cycles. Thus, these natural variability modes can enhance or compensate each other depending on the time period.

Recent studies for the modern warming period argue that a combination of a strongly negative PDO phase contrary to a moderately positive AMO phase is able to slowdown the anthropogenic warming in the early 21st century in the NH (Steinman et al., 2015). This is due to a weakening of the temperature difference between the equator and the pole and a corresponding decrease of the NH westerlies. At the same time, in some experiments with CMIP5 general circulation models (Stolpe et al., 2017) changes in global warming rates within the 20th century still persist after removing the influence of the AMO and PDO, and the contribution of the internal variability in the two oceans to the

modern global warming is estimated to be less than 10%. Furthermore, the study (Haustein et al., 2019) using various observations and historical climate simulations from CMIP5 models, declares that internal multidecadal ocean variability was an unlikely driver of global SAT changes in the 20th century highlighting external forcing as a major cause, including the hypothesis that multidecadal North Atlantic SST variations are also primarily controlled by anthropogenic aerosol forcing.

In order to estimate potential contribution of major natural variability indices, namely AMO, PDO, NAO and PNA, to long-term winter Arctic SAT variations, we used multiple regression analysis. Fig. 10 shows the Arctic SAT as observed and calculated from linear relationships to AMO, PDO, NAO and PNA indices in frame of multiple linear regression model. The results suggest that ocean and atmosphere internal variability may explain a considerable part of the observed SAT variations including the early warming period, while for the period of the modern warming until 2010, this factor has a lower impact (Fig. 10). It should be noted that the AMO variability contributes the major part.

The explained variance by this regression model amounts to 39.1% over the 110-year period, with 33.7% allocated to AMO, 0.3% to PDO, 1.5% to NAO and 3.6% to PNA that indicates a predominant role of the multi-decadal North Atlantic SSTs variations in the Arctic SAT variations in the 20th century.

Thus, given the assumptions of purely internal origin and independence, it can be suggested that large-scale internal climate variability in the North Atlantic is one of the most plausible mechanisms that may explain a major part of ETCW. In recent years, there have been a number of studies highlighting the Pacific Ocean as a source of long-term climate fluctuations, both on global scale and in high latitudes (e.g., Svendsen et al., 2018; Tokinaga et al., 2017; Wegmann et al., 2017). The relative contribution of the Atlantic and Pacific sectors in ETCW event still remains a matter of debates. Furthermore, a number of model experiments (Yamanouchi, 2011; Shiogama et al., 2006; Delworth and Knutson, 2000) argue that the internal variability as a single factor cannot explain the entire amplitude of ETCW SAT fluctuations and must be supplemented by external forcings. Better constrained data reconstructions for the early 20th century period and coordinated climate model simulations are required to disentangle relative contribution from different natural variability factors.

Of course, this regression model is idealized and based on the assumptions that these variability modes are not influenced by external forcing and independent from each other. Given presumably a natural origin of the used variability modes, such an assumption can be taken as a null-hypothesis, although there are studies indicating that these variability modes are inter-related and/or affected by external forcing (e.g.,

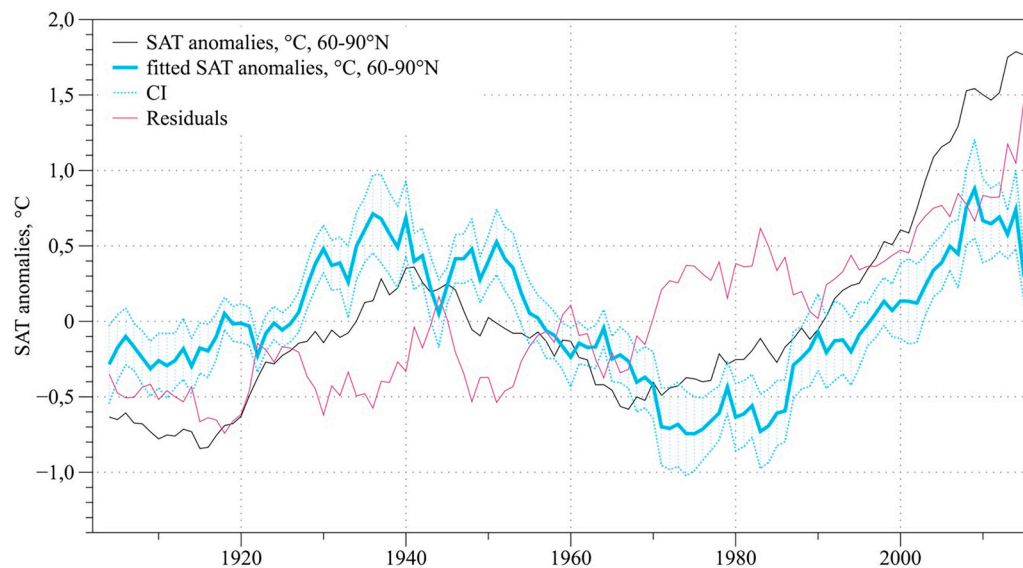


Fig. 10. Annual Arctic (60–90°N) SAT anomalies, (°C) for 1900–2010 (black curve), multiple regression model of winter Arctic SAT onto AMO, PDO, NAO and PNA indices (blue line), residuals (pink line), confident interval (CI, blue dashed area); according to Berkley dataset. The reference period for temperature anomalies is 1951–1980, 7-year running mean. (For interpretation of the references to colour in this figure legend, the reader is referred to the web version of this article.)

Deser et al., 2004; Latif et al., 2006; d’Orgeville and Peltier, 2007; Booth et al., 2012). A relatively short period (about 100 years) of reliable observations in the northern high latitudes contains at most a couple of multidecadal AMO cycles. This hinders statistical analysis of possible linkages based purely on empirical data. Although modelling studies and studies using paleo-reconstructions suggest that multidecadal climate variability in the Arctic and North Atlantic are related during multi-centennial periods (e.g., Semenov, 2008; Miles et al., 2014), there are indications that the multidecadal climate variations in the Arctic are irregular and are not a part of quasi-periodic cycles (Wood et al., 2010).

3.3. Positive feedbacks in the Arctic climate system

The climate system sensitivity to external forcing, for example, to an increase of GHG in the atmosphere, depends on whether and how the response is linked to the processes in the affected system that may add to or reduce the initial forcing thus forming a feedback. Feedbacks are key elements in the Earth climate system that can mitigate or accelerate climate changes and generate climate cycles (e.g., Roe, 2009). Feedbacks that contribute to the accelerated Arctic warming include the following processes: increased absorption of solar radiation due to a decrease of surface albedo as a result of sea ice and snow melt; enhanced greenhouse effect as a result of increased water vapor concentrations due to increased water holding capacity of the warmer air; increased cloud cover due to higher humidity in winter time that may also contribute to enhanced greenhouse effect, but in summer time, it also leads to negative feedback by reflecting incoming solar radiation (clouds feedback also critically depend on cloud types); radiative Planck and lapse rate feedbacks; changes in the carbon cycle, such as the increased release of CO₂ and methane from the land ecosystems and sea shelves as a result of melting permafrost and methane hydrates release; dynamical feedbacks in the ocean and atmosphere leading to increased heat transport to the Arctic (Pithan and Mauritsen, 2014; Bengtsson et al., 2004).

Positive feedbacks amplify climate response to the initial forcing (e.g., radiation forcing due to CO₂ growth), while negative feedbacks act to reduce the response. In particular, positive temperature – water vapor feedback roughly triples surface air temperature sensitivity to changes of CO₂ concentration in the atmosphere (Roe, 2009). Surface air temperature – surface albedo feedback increases temperature response to the doubling of the CO₂ by 10% (Kattsov et al., 2008). One of the largest

uncertainties in model estimates of climate sensitivity to external forcing is related to the cloud-radiation feedbacks. Cloud characteristics in the northern high latitudes are found to be strongly correlated with the Arctic Sea ice concentrations and atmospheric circulation indices (Chernokulsky and Esau, 2019). An increasing low-level cloud cover leads to enhanced scattering of solar radiation back to space, appearing as a negative feedback, but in case of high-level clouds are also able to retain the terrestrial longwave radiation, contributing to the greenhouse effect (e.g., Kato et al., 2008).

The major well-known negative feedback is the increase of infrared terrestrial radiation into space as the surface warms. According to the Stefan-Boltzmann law, the emitted black-body radiation is a function of the absolute temperature to the fourth power (Stefan, 1879). This requires a stronger temperature increase at lower temperatures that is needed to compensate a given disbalance with downward radiation that may also contribute to AA.

High uncertainty of a particular feedback contribution to the observed temperature changes (especially the cloud – radiation feedback and feedbacks related to carbon cycle) is the main cause of a wide spread of global warming projections estimated by climate models. Regional dynamical and radiation feedbacks contribute significantly to the Arctic climate change, and can both amplify or mitigate the external forcing and internal variability. The retreat of the Arctic Sea ice cover as a result of enhanced ocean heat transport from the North Atlantic leads to a heating of the lower atmosphere and generation of ascending air flows in the regions of newly open water, what consequently causes a pressure decrease and circulation changes including a growth of cyclonic activity (Zolotokrylin et al., 2014; Akperov et al., 2020). Such changes may lead to a further enhanced oceanic inflow amplified by westerly and southwesterly winds (Bengtsson et al., 2004). This leads to even greater sea ice reduction. The described mechanism illustrates a positive feedback that involves the Arctic atmosphere circulation and, consequently, affects the climate variations (Chen et al., 2018).

The important geographic feature of the Arctic is the semi-closed Arctic Ocean that connects to the global ocean basically in the Atlantic sector by two major flows: though the Fram Strait and Barents Sea opening. Whereas warm and salty Atlantic water entering Fram Strait at several hundred meters depth does not effectively exchange heat within the upper ocean layer and atmosphere (this situation, however, seems to change in the recent years (Ivanov et al., 2018)), in the shallow Barents Sea, it loses about 90% of the transported heat to the

atmosphere thus directly determining regional air temperature and circulation variability (Smedsrud et al., 2013). Barents Sea accounts for about 10% of the Arctic Ocean area, but despite its relatively small size it is a key region for ocean heat release to the Arctic atmosphere (Schlichtholz, 2013). The most intensive sea ice decline in the Barents Sea was observed recently, in particular due to the intensification of ocean and atmosphere heat fluxes from low latitudes (Smedsrud et al., 2013). Barents Sea is one of the largest contributors to the March sea ice extent loss since 1979 in the Northern Hemisphere (27%) along with the fact that this region is virtually free of ice in summer season within last decade (Onarheim et al., 2018). There are indication from observational data that September sea ice area in the Barents Sea was anomalously low (close to zero in some years) during ETCW period (Zakharov, 2003; Alekseev et al., 2009). The reduction of sea ice concentrations in cold season caused by the enhanced oceanic inflow may trigger changes in regional atmosphere circulation favor further enhanced inflow to Barents Sea thus forming a positive feedback that was suggested to be a mechanism for ETCW (Bengtsson et al., 2004).

Thus, intensified temperature changes in the Arctic could be, in particular, initially triggered by fluctuations of regional atmosphere-ocean dynamics and then significantly enhanced by positive feedbacks within the Arctic climate system. Such amplified Arctic climate changes may in turn affect temperature change both on regional and even global scale, e.g., reducing equator-pole temperature gradient and meridional heat transport (Semenov et al., 2010).

4. Contribution from natural external forcings

4.1. Solar activity

The evidence of a noticeable climate response to changes in solar activity is seen in instrumental and proxy data. Statistically significant correlations between regional and large scale climate characteristics including SAT and solar radiation activity were revealed on different time scales (see, e.g., Reid, 1997; Mokhov and Smirnov, 2008; Hathaway, 2015).

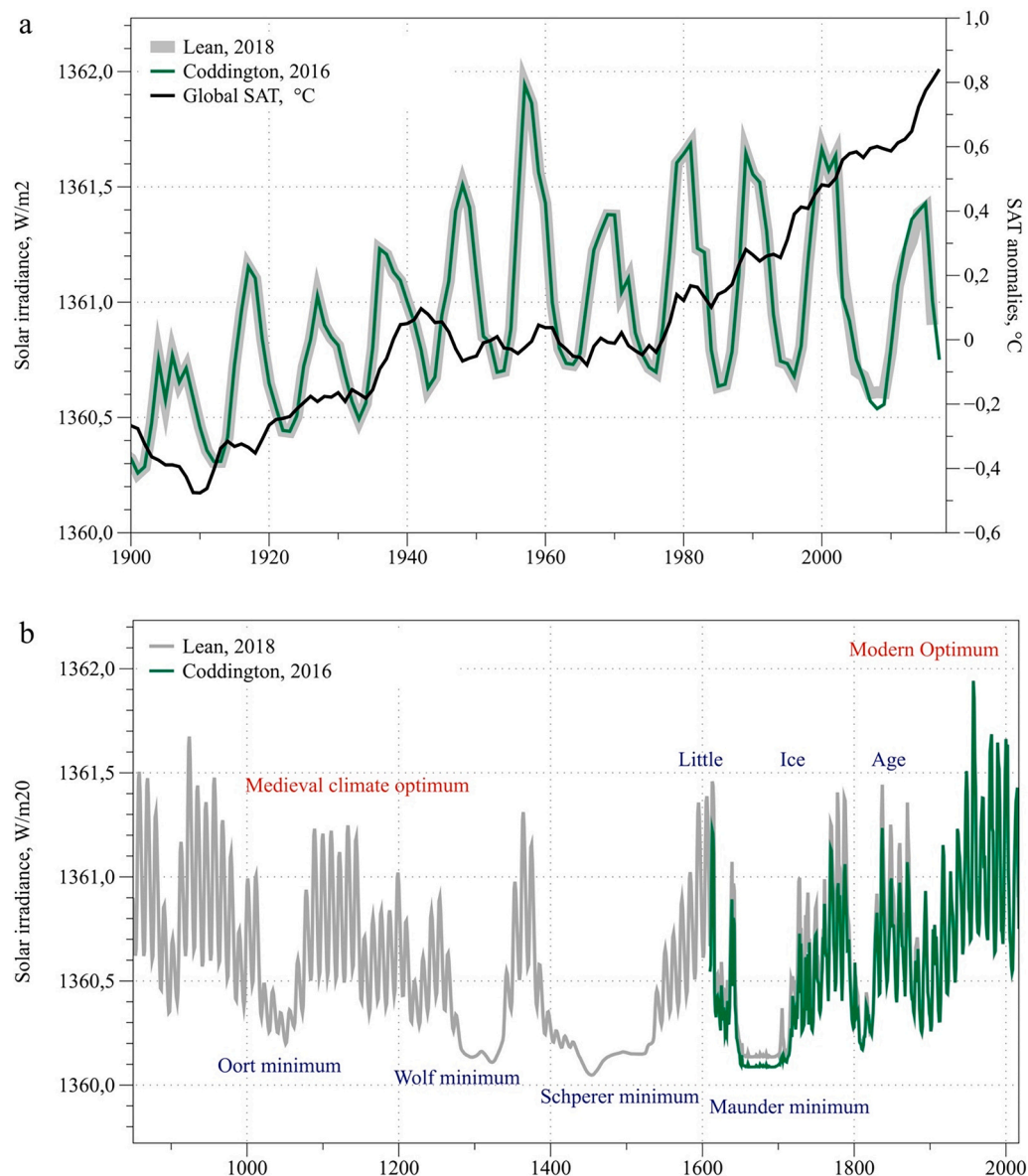


Fig. 11. a, b. Total solar irradiance (W/m²) reconstructions since 1900–2018 (a) and from 850 to 2018 (b) according to reconstructions: Lean, 2018 (gray curve); Coddington et al., 2016 (green curve); and global SAT anomalies (a), °C (black curve) according to Berkley dataset. The reference period for temperature anomalies is 1951–1980, 5-year running mean.

One of the problems with assessing the links between solar exposure and climate is a relatively short length of the currently available direct satellite data, covering only a period of several decades since 1978. This is not enough to identify centennial or multi-decadal trends, though data from earlier time period are based on various reconstructions, that may contain considerable uncertainties and inconsistencies (Suo et al., 2013). The latter multi-century reconstructions for total solar irradiance from 850 CE based on solar irradiance models demonstrate minor discrepancies during the last centuries, including the ETCW period (Fig. 11 a, b; Coddington et al., 2016; Lean, 2018).

One of the most striking historical examples of the impact of solar irradiance on global temperatures is the major cooling period in Europe, the Little Ice Age in 14th–19th centuries, a period with the absence of the anthropogenic factor and coincided with a relatively weak solar activity period (Fig. 11b). In particular, negative SAT anomaly in the second half of the 17th – beginning of the 18th century was accompanied by the minimum of solar activity – the event called the Maunder Minimum (Eddy, 1976). However, many studies indicate that even such a strong decrease of solar radiation does not explain the full amplitude of the medieval cooling. A contribution from other forcing factors such as unusually high volcanic activity (Owens et al., 2017), as well as internal climate fluctuations was suggested. For example, the simulation with a coupled atmosphere-ocean model (Zorita et al., 2004) reveals a significant weakening of the strength of the ocean Gulf Stream current in the North Atlantic and Kuroshio current in the North Pacific transporting heat from low to high latitudes in the NH (Zorita et al., 2004). Furthermore, the Little Ice Age could be a regional phenomenon and did correspond to the global temperature anomaly (Mann, 2002).

The relative role of solar activity that might have caused 20th century climate fluctuations is a subject of various assessments. Early results by Reid (1997) based on one-dimensional ocean model calculations forced by a solar irradiance reconstruction suggest that anthropogenic and solar forcing could equally contribute to the global SAT changes from 1900 to 1955 stating the underestimation of the importance of solar irradiance. Applying a statistical model of information transfer between solar flare intermittency and Earth temperature variations, Scafetta and West (2008) assigned 69% of surface temperature variance in 20th century to the solar activity, however their approach was argued to be flawed (Rypdal and Rypdal, 2010). Multiple regression analysis by Lean and Rind (2008) based on observational data suggests that solar forcing contributed only 10% to global warming from 1905 to 2005 and resulted in negligible long-term warming in 1980–2005. According to Mokhov and Smirnov (2008), the empirical analysis of several solar reconstructions shows that the solar activity may only explain 8% of the global SAT variability in 1897–1936 period and 27% in the second half of the 20th century. Przybylak et al. (2020) made an inventory of solar radiation measurements in the Arctic during the ETCW (1921–50) period and, though not making quantitative assessments, distinguished a brightening phase during 1921–1950 period followed by a stabilization phase (1951–93), and a dimming phase (after 2000). In general, the analysis of empirical shows a relatively minor role of solar activity in the SAT variability during ETCW period. Still, according to model experiments intensified solar radiation could cause more warming in the early warming period than anthropogenic factor (Nozawa et al., 2005) and along with low volcanic activity during the 1920s–1950s could be a significant cause of the Early 20th Century Warming in the Arctic (Suo et al., 2013). However, this factor may not explain the ETCW event alone.

Thus, the role of solar activity is controversial, its contribution is most likely relatively small and should be reinforced with further external forcing and internal natural variability.

4.2. Volcanic activity

The climate system response to external factors can be determined from empirical data including paleo reconstructions and by climate

model simulations, which suggests that the impact of volcanic aerosols on climate, particularly on interannual to multi-decadal time scale, is considerably larger than the solar activity (Owens et al., 2017).

Sulfur dioxide as a part of volcanic gases released during the eruption, produces sulphate aerosol particles when reacting with water in the atmosphere. The latter when brought to the stratosphere by strong volcanic injections are not removed by precipitation processes and may remain there several months spreading from the eruption spot to around the globe within several weeks. Sulfate aerosols reflect solar radiation and increase the planetary albedo (Sigurdsson, 1990). It has a negative effect on the Earth's radiation balance leading to a global SAT decrease by a few tenths of a degree Celsius within several months after the major volcanic eruptions. This effect may persist, depending on the eruption strength, for several years due to thermal inertia of the cooled oceans (Robock, 2000; Mass and Portman, 1989).

In the second half of the 20th century, actinometric measurements revealed that the presence of volcanic aerosols in the stratosphere reduces incoming short-wave radiation at polar latitudes by 5–7% for 1–3 years after the eruption (depending on its strength) (Mass and Portman, 1989).

Volcanic activity during the 20th century measured by the aerosol optical depth (AOD) is presented in Fig. 12. AOD is a quantitative estimate of aerosol present in the atmosphere that measures the extinction of a ray of light due to absorbing or scattering processes as it passes through the atmosphere (Sato et al., 1993). It can be seen that the strongest volcanic impact on AOD leading to negative radiation forcing has been observed before 1920s and after 1960s. The effect of volcanic eruptions on inter-decadal time scales leads to a global surface temperature variations of about 0.1 °C (Eliseev and Mokhov, 2008). After major eruptions in the early 20th century (Santa Maria in 1902, Ksudach in 1907 and Katmai in 1912 (Mass and Portman, 1989), which caused NH SAT decrease on the order of 0.2° to 0.5 °C for periods from one to five years (Self et al., 1981), there was a pause in major volcanic eruptions until 1963 when the Mount Agung eruption occurred. The active volcanism hiatus during 1920s–1950s led to a decrease of sulphate aerosols in the stratosphere and atmosphere optical thickness. This could contribute to ETCW but is not consistent with the subsequent SAT plateau since 1950s.

Volcanic aerosols can for several years compensate or even reverse the SST rise induced by increasing greenhouse gas concentrations (Delworth et al., 2005) and also lead to rapid changes in ocean heat content and sea level. As a result of Pinatubo eruption, the decrease of the ocean heat content amounted to approximately 3×10^{22} J with a drop of the global sea level by 5 mm approximately (Church et al., 2005). Volcanic eruptions may also affect ocean circulation, in particular AMO, primarily due to cooling of the tropical SSTs and changing the thermohaline circulation in the North Atlantic (Otterå et al., 2010). The AMO is associated with a strength of the northward oceanic heat transport that, in turn, influences climate in the Northern Extratropics and in the Arctic (e.g., Semenov et al., 2010).

The uncertainty of estimates of the volcanic aerosols impact on global SAT is related to the fact that spatiotemporal dynamics of volcanic aerosol depends on strength and geological type of an eruption, aerosol chemical composition, along with the season and geographical location (Kravitz and Robock, 2011). This makes it difficult to specify realistically the volcanic aerosol forcing in climate models. In case of a low latitude eruption, a cooling is more pronounced in the polar regions than in the tropics, as it was after the eruption of Mount Agung in 1963 (Viebrock and Flowers, 1968). That event was accompanied by a 7% decrease in total short-wave solar radiation at the South Pole during the first year after the eruption, while the disturbance of total radiation in tropical latitudes barely rose above the noise level (Dyer and Hicks, 1965).

Analysis of SAT sensitivity to external natural factors based on coupled climate model simulations of 20th century climate suggests that the increased solar radiation, together with a pause in major volcanic

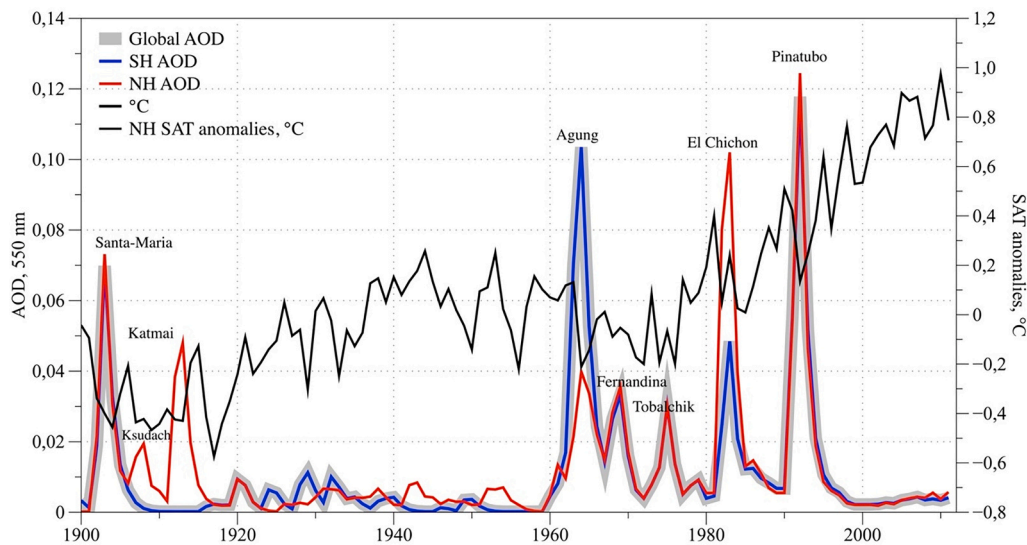


Fig. 12. Average aerosol optical depth (AOD, wavelength at 550 nm) during the 20th century according to the volcanic aerosol forcing used in GISS Climate Model for CMIP5 simulations (Miller et al., 2014) – Global (gray curve); NH (red curve); SH (blue curve) and NH SAT anomalies, °C (black curve), according to Berkley dataset. The reference period for temperature anomalies is 1951–1980 (For interpretation of the references to colour in this figure legend, the reader is referred to the web version of this article.)

eruptions in the 1930s and 1950s, could have caused a significant contribution to ETCW (Suo et al., 2013; Nozawa et al., 2005). However, these factors are insufficient to explain the whole magnitude of the early warming and must be supplemented with other factors, such as internal climate variability, variations of anthropogenic GHG and aerosols.

5. Mechanisms: anthropogenic forcing

5.1. Anthropogenic aerosols

While variations of solar and volcanic activity cannot explain the ETCW magnitude alone (Nozawa et al., 2005; Shioyama et al., 2006; Suo et al., 2013) – some studies suggest that external anthropogenic factors, such as an increase of GHG could have had an equal contribution to the ETCW SAT increase along with solar forcing (Reid, 1997). Deviations from gradual global warming caused by increasing concentrations of GHG in the atmosphere may be associated with changes in anthropogenic aerosols emissions (Shindell and Faluvegi, 2009). Analysis of historical single- and all-forcing simulations from CMIP5 climate models' ensemble suggest that anthropogenic aerosols were a major driver of mid-latitude Eurasian summer temperature trends throughout the 20th century and explained more than a half of the interdecadal variability of European temperature during 1940–70 (Undorf et al., 2018).

The anthropogenic aerosols forcing of the global climate is a concept intensively discussed over past decades (Haywood and Boucher, 2000; Shindell and Faluvegi, 2009; Booth et al., 2012; Undorf et al., 2018). A response of climate system to anthropogenic aerosols is highly uncertain due to spatially heterogeneous and time dependent forcing patterns and their direct and indirect impacts on atmospheric reflectivity (Haywood and Boucher, 2000; Chylek et al., 2016a, 2016b). Furthermore, some recent studies suggest an indirect aerosol effects through a possibility of aerosol impact on oceanic circulation variability in the North Atlantic with important implications for the global climate (e.g., Booth et al., 2012; Suo et al., 2013). These results, however, are disputed by Zhang et al. (2013).

Aerosols vary in their characteristics and may have opposite effects on surface temperature. The direct aerosol effect is caused by either scattering or absorption (depending on aerosol type) of solar radiation, when sulfate, nitrate, organic aerosol or water vapor particles scatter incoming solar radiation and lead to a negative radiative forcing (Takemura et al., 2005). In contrast, aerosol carbon particles, i.e., soot (“black carbon”) mainly absorb radiation, resulting in a positive radiative forcing and warming of the low troposphere (McConnell et al.,

2007). Such a heating may have a pronounced effect on the atmospheric stability leading to changes in convection and consequently affecting large scale circulation and hydrological cycle, leading to significant regional and remote climatic effects (Menon et al., 2002).

The main uncertainty in assessing the impact of anthropogenic aerosols is related to their indirect effect, wherein aerosols particles affect the climate system through changes in cloud optical properties (Takemura et al., 2005). The indirect effect, in turn, can be divided into two major categories. The first one is an increase of the number and decrease of the effective radius (size) of cloud condensation nuclei (droplets) caused by increasing concentrations of aerosol particles. This results in a larger cloud surface area and enhancement of cloud reflectivity (Twomey, 1974) – called Twomey effect. The second effect manifests itself in a longer lifetime of clouds, because the reduction of the effective radius of cloud droplets slows down formation of precipitation (Albrecht, 1989). More clouds with longer lifetime increase the planetary albedo, thereby contributing to the surface cooling and may largely compensate the global warming caused by greenhouse effect (Quaas et al., 2008). But aerosol-cloud interaction is dependent on different cloud types, including the case of contact with supercooled cloud droplets, when aerosols can act as ice nuclei, initiating freezing that leads to a rapid glaciation of the cloud and reduction of cloud lifetime, cover and optical depth that leads to more absorption of solar radiation by the Earth climate system (Lohmann and Feichter, 2005).

The analysis of the CMIP5 climate model experiments suggests that up to 60% of the global warming during the entire 20th century caused by GHG could be compensated by the climate system response to other anthropogenic aerosols. Without such a compensating effect, the Arctic region would have experienced a stronger, by 1.8 °C, warming throughout the 20th century (Najafi et al., 2015). Other experiments (Gagné et al., 2017) demonstrate that aerosol forcing could postpone the Arctic sea ice cover decline in 1950–1975 period due to GHG impact. At the same time, another study based on CMIP5 climate models' simulations showed that the Arctic temperature variations during the 20th century are equally well reproduced in simulations with and without full indirect aerosol effect (Chylek et al., 2016a, 2016b).

Direct and indirect aerosol effects on radiation balance are complemented by the impacts on atmospheric circulation through cooling or heating different parts of atmosphere (both in horizontal and vertical dimensions). Assessment of these impacts is even more uncertain. Analysis of internal modes of atmospheric variability in a climate model (Gillett et al., 2000) shows that the Arctic Oscillation, which significantly impacts atmospheric heat transport to the Arctic, does not exhibit a statistically significant response to GHG, sulphate aerosols or ozone

forcing. At the same time, other modelling studies (e.g., [Shindell and Faluvegi, 2009](#)) indicate an important role of aerosols in shaping regional climate trends including accelerated modern warming in the Arctic. The discrepancy of the results may also be related to model's resolution, advance in development and simulations' setup.

The Arctic climate is also sensitive to the positive radiative forcing effect of the black carbon (BC) aerosols, which have a serious impact on physical and chemical properties of the atmosphere and underlying surface ([Koch and Hansen, 2005](#)). BC is commonly known as soot that is emitted by burning fossil fuels and biomasses. The highest concentrations of black carbon and its impact on the climate are observed primarily in the Northern Hemisphere ([Fig. 13](#)), where the percentage of land area is higher, most of the world population lives and, as a consequence, the bulk of industrial production is located.

Soot particles reduce the snow and sea ice albedo. Annually averaged albedo decrease amounts to 1.5% for the Arctic and 3% for the NH that results in the increase of radiative forcing by 0.3 W/m^2 in the Northern Hemisphere in the 20th century ([Hansen and Nazarenko, 2004](#)). Such an effect also suggests a positive feedback – stronger and earlier snow melt may lead to more BC aerosols emissions. Furthermore, it causes changes of hydrological cycle ([Koch and Hansen, 2005](#)) and impact cloud cover ([Twomey, 1974](#)) thus affecting atmospheric stability and circulation in the Arctic region.

According to the analysis of the ice cores from Greenland, the maximum BC concentration in the Arctic during the 20th century was observed from 1906 to 1910 ([McConnell et al., 2007](#)) followed by a minor decline through the late 1940s and a sharp fall in 1950s that is partly consistent with the forcing prescribed in CMIP5 model ensemble ([Fig. 13](#)). This suggests a possible contribution of the black carbon forcing to ETCW.

Anthropogenic aerosol contribution to the global and regional climate changes over the past century could be a significant factor and, as noted above, could partly compensate the positive radiative forcing of GHG, but its quantitative estimates are strongly uncertain due to the direct and indirect effects on radiation balance and possible changes in atmospheric and even ocean circulation resulting in non-linear and remote climate changes.

5.2. Greenhouse gases

The anthropogenic increase of greenhouse gases has been a major driver of the observed global and hemispheric temperature changes over the past 50 years ([Bindoff et al., 2013](#)). A contribution of GHG to the mid

20th century warming is, however, uncertain, as the rapid growth of GHG concentrations began after the 1940s ([Fig. 14](#)). Concentrations of carbon dioxide in the Earth's atmosphere from 1979 to 2019 increased from 336 to 411 particles per million (ppm) due to anthropogenic emissions, which is about 60% of the total increase from pre-industrial values in 1850 (286 ppm) to the present time. The increase of CO_2 concentration over the period of 1906–1945 was only 10% (from 299 to 311 ppm; [Tans and Keeling, 2020](#); [MacFarling Meure et al., 2006](#)) and cannot explain ETCW alone. Furthermore, despite a slowdown of GHG concentration increase in 1940s–1950s, they continued to rise during this period, which was not consistent with the concurrent global and, particularly, Arctic cooling ([Bengtsson et al., 2004](#)).

Thus, the relatively slow rates of increase in GHG concentrations in the warming phase of ETCW do not agree with SAT variations in the middle of the 20th century, whereas levelling off GHG concentrations in 1940s and 1950s ([Fig. 14](#)) could be a part factor in the Arctic cooling given increasing anthropogenic aerosols load in that period. However, according to climate model simulations, the warming of 1920s–1930s could be a result of the sum of the forcings, including anthropogenic factor ([Stott et al., 2000](#)).

Experiments with a coupled climate model ([Delworth and Knutson, 2000](#)) suggest that the global Early 20th Century Warming could have occurred due to a combination of anthropogenic radiation forcing and internal climate variability. A study by [Meehl et al. \(2004\)](#) shows that reproduction of the warming in the first half of the 20th century requires a combination of solar and anthropogenic factors, whereas radiation forcing due to the increase of GHG is dominant factor for the modern warming period climate response. Similar conclusion was made based on quantitative assessment of four possible external forcing factors radiation and stratospheric volcanic aerosols, and external anthropogenic – GHG and sulphate aerosols) using climate model simulations ([Tett et al., 1999](#)). It was concluded that external natural and anthropogenic forcings were equally important for driving ETCW. More recent climate model simulations ([Suo et al., 2013](#)) demonstrate that it was a combination of external natural and anthropogenic factors that contributed to Arctic temperature changes during early warming with a major part attributed to the natural forcing in this period. These conclusions are supported with an analysis ([Hegerl et al., 2018](#)) with the estimation that almost a half (40–54%) of the global warming in the first half of the 20th century was forced by a combination of increasing anthropogenic and natural forcings.

Thus, the role of the GHG in ETCW period may not be dominant. However, the contribution of GHGs is noticeable in comparison to

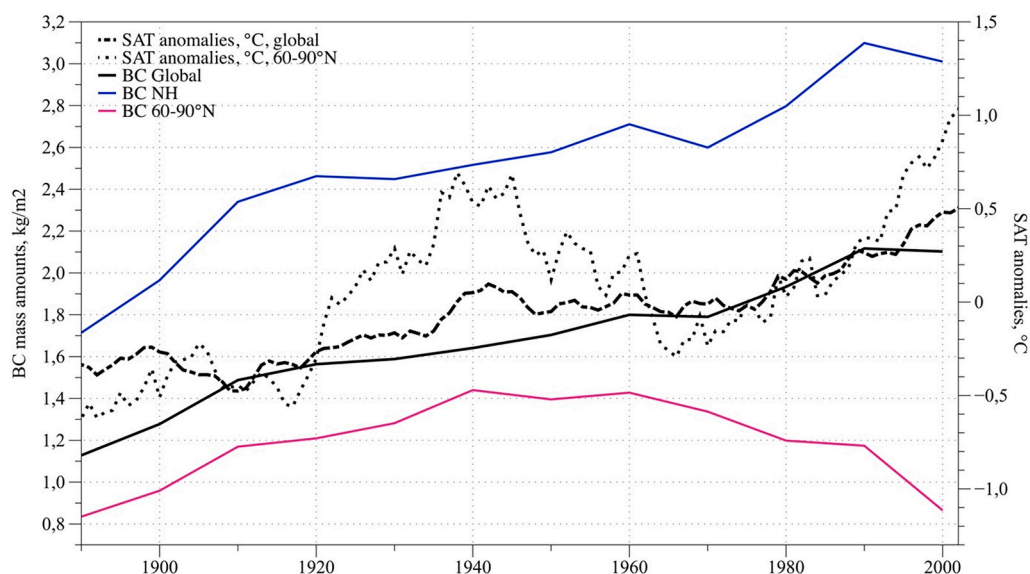


Fig. 13. Industrial black carbon (BC) mass amounts (kg/m^2) for the 20th century as globally averaged (black curve), for the NH (blue curve), for the Arctic ($60\text{--}90^\circ\text{N}$) (pink curve) in the 20th century according to forcing in GISS Climate Model for CMIP5 ([Miller et al., 2014](#)) and global/Arctic SAT anomalies, $^\circ\text{C}$ (black dashed/black dotted), according to Berkley dataset. The reference period for temperature anomalies is 1951–1980, 5-year running mean. (For interpretation of the references to colour in this figure legend, the reader is referred to the web version of this article.)

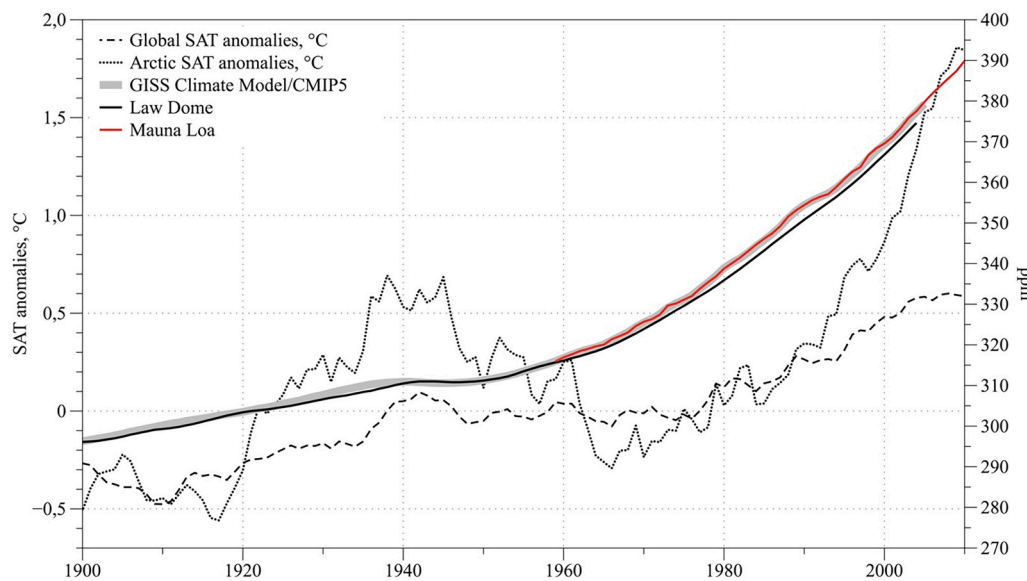


Fig. 14. Concentrations of carbon dioxide in the atmosphere (ppm) for 1860–2015 according to forcing in CMIP5 climate model ensemble (Miller et al., 2014; thick gray line), Antarctic ice core CO₂ reconstructions (Etheridge et al., 1998; black line) and observational data at Mauna Loa (Tans and Keeling, 2020; pink line), and global SAT anomalies, °C (dashed line), according to Berkley dataset. The reference period for temperature anomalies is 1951–1980, 5-year running mean. (For interpretation of the references to colour in this figure legend, the reader is referred to the web version of this article.)

external natural factors and internal climate variability.

6. Discussion and conclusions

The current review focuses on existing hypotheses that account for the Arctic warming in the early 20th century period and discusses studies with analysis of the plausible mechanisms of internal and external climate variability during this warming event.

The Early 20th Century Warming in the Northern Extratropics is comparable to the modern warming in terms of warming rates but happened during the period when the total increase of GHG in the atmosphere from pre-industrial values had been 50% less than in the last 40 years. These rules out the greenhouse forcing as a major driving factor for ETCW and suggests other climate variability mechanisms both of internal (natural) origin and related to external natural and anthropogenic forcings. Understanding mid-century warming mechanisms is a key to determining the relative contribution of internal natural variability and external forcing to global and regional climate changes during the last century including the modern warming period.

The amplitude of ETCW in the Arctic was approximately two to three times (depending on a period and geographical definitions) higher than that averaged for the Northern Hemisphere. Such enhanced long-term regional temperature fluctuations can be both a response to the global climate changes enhanced by a number of regional radiation and dynamical positive feedbacks and can originate internally in the Arctic climate system with a possible feedback to the global temperature changes.

Major mechanisms that may contribute to ETCW include natural internal variability, external natural forcings such as solar irradiance and volcano activity, and external anthropogenic impact due to changing concentrations of aerosols of different nature, and GHG.

Despite the fact that solar irradiance is the major driver affecting Earth's surface temperature variations, its contribution, according to various reconstructions and model experiments, is estimated to be relatively small and alone cannot explain the early climatic fluctuation. The pause in major volcanic eruptions after Katmai eruption in 1915 could have also contributed to the warming in 1920s–1930s. However, the results of climate model experiments demonstrate that even though solar and volcanic activity arguably have a significant impact they are unable to explain the full amplitude of temperature fluctuation during ETCW and should be supplemented with further external forcing and internal variability.

The anthropogenic aerosol forcing has been a thoroughly discussed

concept in the recent studies. Aerosol's concentration changes could possibly alter the evolution of the Arctic SAT over the past century, but still the quantitative estimates of its contribution to ETCW remain the most uncertain. Due to different physical mechanisms including direct and indirect radiative effects, aerosols are able to partly compensate or, on the contrary, enhance the positive radiative forcing caused by growing CO₂. Some studies based on station data in the Arctic suggest a partial contribution of the black carbon effect on snow to ETCW. The concentrations of the latter according to some estimates were growing in the first half of the 20th century.

Some studies suggest that the warming during the early 20th century period may have been partially caused by the increase of GHG. This forcing is unlikely to be the major driving factor as the intensive growth of GHG concentrations has begun after 1950, although it could likely play a role in some extreme climate events in the 1930s. CO₂ increase has been three to four times slower during the early warming if compared to the last three decades of the 20th century, with comparable rates of temperature increase. Feasible estimates based on climate model studies attribute almost a half of the global warming in the first half of the 20th century to a combination of anthropogenic and natural external factors.

According to this overview, the natural internal variability is the most likely mechanism that may explain a major part of ETCW, where the SAT anomaly variations are forced by disposition of major atmospheric and ocean circulation modes. In the period of the modern warming, leading atmosphere variability modes in the Northern Hemisphere (NAO, AO and PNA) could explain more than 40% of the temperature variations in the NH high latitudes, whereas the ocean internal long-term variability seem to be a major natural variability factor driving ETCW. Recent studies suggest ocean circulation as a source of global and Northern Hemisphere long-term climate deviations from the secular warming trend, but a quantitative assessment of the Atlantic and Pacific sectors contribution to ETCW is under discussion, though the latest studies highlight the more pronounced role of the Pacific Ocean than previously thought. Our estimates based on multiple linear regression analysis suggest that internal variations represented by several major ocean and atmosphere natural variability modes, explains almost 40% of the Arctic SAT anomalies in the 20th century, with a predominant role of the Atlantic Multidecadal Oscillation.

Thus, the early climate anomaly in the Northern Extratropics can be attributed to internal climate variability as a major factor, and enhanced by positive feedbacks in the Arctic, in combination with the effects of external natural and anthropogenic forcing (intensified solar irradiance

with a pause in volcanic activity and increase of GHG). But the exact contribution of each mechanism remains uncertain, due to the lack of instrumental data in polar latitudes in mid-20th century and earlier, diverging climate model results, and unclear role of the aerosols forcing and the processes of their interaction with other components of the climate system.

Declaration of Competing Interest

The authors declare that they have no known competing financial interests or personal relationships that could have appeared to influence the work reported in this paper.

Acknowledgements

The authors are deeply thankful to three anonymous reviewers for their constructive comments that helped us to significantly improve the review. The analysis of climate variability mechanisms was supported by Russian Ministry of Science and Higher Education (Agreement No. 075-15-2021-577), climate model analysis and empirical data evaluation were performed in frame of State Assignment of the Russian Ministry of Science and Higher Education (No. 0148-2019-0009), the Polar amplification analysis was supported by the Russian Foundation for Basic Research (No. 20-55-71003).

References

Akperov, M., Semenov, V.A., Mokhov, I.I., Dorn, W., Rinke, A., 2020. Impact of Atlantic water inflow on winter cyclone activity in the Barents Sea: insights from coupled regional climate model simulations. *Environ. Res. Lett.* 15, 024009 <https://doi.org/10.1088/1748-9326/ab6399>.

Albrecht, B.A., 1989. Aerosols, cloud microphysics, and fractional cloudiness. *Science* 245, 1227–1230. <https://doi.org/10.1126/science.245.4923.1227>.

Alekseev, G.V., Danilov, A.I., Kattsov, V.M., Kuzmina, S.I., Ivanov, N.E., 2009. Changes in the climate and sea ice of the Northern Hemisphere in the 20th and 21st centuries from data of observations and modeling. *Izvestiya Atmos. Ocean. Phys.* 45, 675–686. <https://doi.org/10.1134/s0001433809060012> (2009).

Alexeev, V.A., Langen, P.L., Bates, J.R., 2005. Polar amplification of surface warming on an aquaplanet in “ghost forcing” experiments without sea ice feedbacks. *Clim. Dyn.* 24 (7–8), 655–666. <https://doi.org/10.1007/s00382-005-0018-3>.

Alexeev, V.A., Walsh, J.E., Ivanov, V.V., Semenov, V.A., Smirnov, A.V., 2017. Warming in the Nordic Seas, North Atlantic storms and thinning Arctic sea ice. *Environ. Res. Lett.* 12 (8), 084011 <https://doi.org/10.1088/1748-9326/aa7a1d>.

Allan, R., Ansell, T., 2006. A new globally complete monthly historical gridded mean sea level pressure dataset (HadSLP2): 1850–2004. *J. Clim.* 19 (22), 5816–5842. <https://doi.org/10.1175/JCLI3937.1>.

Ambaum, M.H., Hoskins, B.J., Stephenson, D.B., 2001. Arctic oscillation or North Atlantic oscillation? *J. Clim.* 14 (16), 3495–3507. [https://doi.org/10.1175/1520-0442\(2001\)014<3495:AONAO>2.0.CO;2](https://doi.org/10.1175/1520-0442(2001)014<3495:AONAO>2.0.CO;2).

Arrhenius, S., 1896. XXXI. On the influence of carbonic acid in the air upon the temperature of the ground. *The London, Edinburgh, Dublin Philos. Mag. J. Sci.* 41 (251), 237–276. <https://doi.org/10.1080/14786449608620846>.

Barnston, A.G., Livezey, R.E., 1987. Classification, seasonality and persistence of low-frequency atmospheric circulation patterns. *Mon. Wea. Rev.* 115 (6), 1083–1126. [https://doi.org/10.1175/1520-0493\(1987\)115<1083:CSAPOL>2.0.CO;2](https://doi.org/10.1175/1520-0493(1987)115<1083:CSAPOL>2.0.CO;2).

Bekryaev, R.V., Polyakov, I.V., Alexeev, V.A., 2010. Role of polar amplification in long-term surface air temperature variations and modern Arctic warming. *J. Clim.* 23 (14), 3888–3906. <https://doi.org/10.1175/2010JCLI3297.1>.

Bengtsson, L., Semenov, V.A., Johannessen, O.M., 2004. The early twentieth-century warming in the Arctic—a possible mechanism. *J. Clim.* 17 (20), 4045–4057. [https://doi.org/10.1175/1520-0442\(2004\)017<4045:TETWIT>2.0.CO;2](https://doi.org/10.1175/1520-0442(2004)017<4045:TETWIT>2.0.CO;2).

Bindoff, N.L., Stott, P.A., AchutaRao, K.M., Allen, M.R., Gillett, N., Gutzler, D., Hansing, K., Hegerl, G., Hu, Y., Jain, S., Mokhov, I.I., 2013. Detection and Attribution of Climate Change: From Global to Regional.

Bokuchava, D.D., Semenov, V.A., 2018. Analiz anomalij prizemnoj temperatury vozduha v Severnom polusharii v techenie XX veka po dannym nabljudenij i reanalizov [Analysis of surface air temperature anomalies in the Northern Hemisphere during the twentieth century according to observational and reanalyses.]. *Fundam. Prikl. Klimatol.* 1, 28–51. <https://doi.org/10.21513/2410-8758-2018-1-28-51>.

Booth, B.B., Dunstone, N.J., Halloran, P.R., Andrews, T., Bellouin, N., 2012. Aerosols implicated as a prime driver of twentieth-century North Atlantic climate variability. *Nature* 484 (7393), 228–232. <https://doi.org/10.1038/nature10946>.

Brennan, M.K., Hakim, G.J., Blanchard-Wrigglesworth, E., 2020. Arctic sea-ice variability during the instrumental era. *Geophys. Res. Lett.* 47 (7) <https://doi.org/10.1029/2019GL086843> p.e2019GL086843.

Brohan, P., Kennedy, J.J., Harris, I., Tett, S.F., Jones, P.D., 2006. Uncertainty estimates in regional and global observed temperature changes: a new data set from 1850. *J. Geophys. Res. Atmos.* 111 (D12) <https://doi.org/10.1029/2005JD006548>.

Brönnimann, S., 2009. Early twentieth-century warming. *Nat. Geosci.* 2 (11), 735. <https://doi.org/10.1038/ngeo670>.

Budyko, M.I., 1969. *Polar Ice and the Climate*. 36. Gidrometeoizdat. Leningrad (in Russian).

Bulygina, O.N., Razuvaev, V.N., Trofimenco, L.T., Shvets, N.V., 2015. *An Array of Data on the Average Monthly Air Temperature at Stations in Russia*. VNIIGMI-MCD, Obninsk (in Russian).

Caballero, R., Langen, P.L., 2005. The dynamic range of poleward energy transport in an atmospheric general circulation model. *Environ. Res. Lett.* 32 (2) <https://doi.org/10.1029/2004GL021581>.

Callendar, G.S., 1938. The artificial production of carbon dioxide and its influence on temperature. *Q. J. R. Meteorol. Soc.* 64 (275), 223–240. <https://doi.org/10.1002/qj.49706427503>.

Chen, H.W., Zhang, Q., Körnich, H., Chen, D., 2013. A robust mode of climate variability in the Arctic: the Barents Oscillation. *Geophys. Res. Lett.* 40 (11), 2856–2861. <https://doi.org/10.1002/grl.50551>.

Chen, L., Francis, J., Hanna, E., 2018. The “Warm-Arctic/Cold-continents” pattern during 1901–2010. *Int. J. Climatol.* 38 (14), 5245–5254. <https://doi.org/10.1002/joc.5725>.

Chernokulsky, A., Esau, I., 2019. Cloud cover and cloud types in the Eurasian Arctic in 1936–2012. *Int. J. Climatol.* 39 (15), 5771–5790. <https://doi.org/10.1002/joc.6187>.

Church, J.A., White, N.J., Arblaster, J.M., 2005. Significant decadal-scale impact of volcanic eruptions on sea level and ocean heat content. *Nature* 438 (7064), 74–77. <https://doi.org/10.1038/nature04237>.

Chylek, P., Klett, J.D., Dubey, M.K., Hengartner, N., 2016a. The role of Atlantic Multidecadal Oscillation in the global mean temperature variability. *Clim. Dyn.* 47 (9–10), 3271–3279. <https://doi.org/10.1007/s00382-016-3025-7>.

Chylek, P., Vogelsang, T.J., Klett, J.D., Hengartner, N., Higdon, D., Lesins, G., Dubey, M.K., 2016b. Indirect aerosol effect increases CMIP5 models’ projected arctic warming. *J. Clim.* 29 (4), 1417–1428. <https://doi.org/10.1175/JCLI-D-15-0362.1>.

Coddington, O., Lean, J.L., Pilewskie, P., Snow, M., Lindholm, D., 2016. A solar irradiance climate data record. *Bull. Am. Meteorol. Soc.* 97 (7), 1265–1282. <https://doi.org/10.1175/BAMS-D-14-00265.1>.

Cohen, J., Screen, J.A., Furtado, J.C., Barlow, M., Whittleston, D., Coumou, D., Francis, J., Dethloff, K., Entekhabi, D., Overland, J., Jones, J., 2014. Recent Arctic amplification and extreme mid-latitude weather. *Nat. Geosci.* 7 (9), 627–637. <https://doi.org/10.1038/ngeo2234>.

Compo, G.P., Whitaker, J.S., Sardeshmukh, P.D., Matsui, N., Allan, R.J., Yin, X., Gleaso, B.E., Vose, R.S., Rutledge, G., Bessemoulin, P., Brönnimann, S., Brunet, M., Crouthamel, R.I., Grant, A.N., Groisman, P.Y., Jones, P.D., Kruk, M., Kruger, A.C., Marshall, G.J., Mauger, M., Mok, H.Y., Nordli, Ø., Ross, T.F., Trigo, R.M., Wang, X.L., Woodruff, S.D., Worley, S.J., 2011. The twentieth century reanalysis project. *Q. J. R. Meteorol. Soc.* 137, 1–28. <https://doi.org/10.1002/qj.776>.

Delworth, T.L., Knutson, T.R., 2000. Simulation of early 20th century global warming. *Science* 287 (5461), 2246–2250. <https://doi.org/10.1126/science.287.5461.2246>.

Delworth, T.L., Mann, M.E., 2000. Observed and simulated multidecadal variability in the Northern Hemisphere. *Clim. Dyn.* 16 (9), 661–676. <https://doi.org/10.1007/s003820000075>.

Delworth, T.L., Ramaswamy, V., Stenchikov, G.L., 2005. The impact of aerosols on simulated ocean temperature and heat content in the 20th century. *Geophys. Res. Lett.* 32 (24) <https://doi.org/10.1029/2005GL024457>.

Deser, C., Phillips, A.S., Hurrell, J.W., 2004. Pacific interdecadal climate variability: linkages between the tropics and the North Pacific during boreal winter since 1900. *J. Clim.* 17, 3109–3124. [https://doi.org/10.1175/1520-0442\(2004\)017<3109:PICVLB>2.0.CO;2](https://doi.org/10.1175/1520-0442(2004)017<3109:PICVLB>2.0.CO;2).

Dommenget, D., 2009. The ocean’s role in continental climate variability and change. *J. Clim.* 22 (18), 4939–4952. <https://doi.org/10.1175/2009JCLI2778.1>.

d’Orgeville, M., Peltier, W.R., 2007. On the Pacific decadal oscillation and the Atlantic multidecadal oscillation: might they be related? *Geophys. Res. Lett.* 34, L23705 <https://doi.org/10.1029/2007GL031584>.

Dyer, A.J., Hicks, B.B., 1965. Radioactive fallout in southern Australia during the years 1958–1964. *J. Geophys. Res.* 70 (16), 3879–3883. <https://doi.org/10.1029/JZ070i016p03879>.

Eddy, J.A., 1976. The maunder minimum. *Science* 192 (4245), 1189–1202. <https://doi.org/10.1126/science.192.4245.1189>.

Eliseev, A.V., Mokhov, I.I., 2008. Influence of volcanic activity on climate change in the past several centuries: assessments with a climate model of intermediate complexity. *Atmos. Ocean. Phys.* 44 (6), 671–683. <https://doi.org/10.1134/S0001433808060017>.

Etheridge, D.M., Steele, L.P., Langenfelds, R.L., Francey, R.J., Barnola, J.M., Morgan, V.I., 1998. Historical CO₂ records from the Law Dome DE08, DE08-2, and DSS ice cores. *Trends* 351–364.

Frolov, I.E., Gudkovich, Z.M., Radionov, V.F., Shirochkov, A.V., Timokhov, L.A., 2006. *The Arctic Basin: Results From the Russian Drifting Stations*. Springer Science and Business Media. <https://doi.org/10.1007/3-540-37665-8>.

Gagné, M.É., Fyfe, J.C., Gillett, N.P., Polyakov, I.V., Flato, G.M., 2017. Aerosol-driven increase in Arctic sea ice over the middle of the twentieth century. *Geophys. Res. Lett.* 44 (14), 7338–7346. <https://doi.org/10.1002/2016GL071941>.

Gillett, N.P., Hegerl, G.C., Allen, M.R., Stott, P.A., 2000. Implications of changes in the Northern Hemisphere circulation for the detection of anthropogenic climate change. *Geophys. Res. Lett.* 27 (7), 993–996. <https://doi.org/10.1029/1999GL010981>.

Graversen, R.G., Wang, M., 2009. Polar amplification in a coupled climate model with locked albedo. *Clim. Dyn.* 33 (5), 629–643. <https://doi.org/10.1007/s00382-009-0535-6>.

Gray, S.T., Graumlich, L.J., Betancourt, J.L., Pederson, G.T., 2004. A tree-ring based reconstruction of the Atlantic Multidecadal Oscillation since 1567 AD. *Geophys. Res. Lett.* 31 (12) <https://doi.org/10.1029/2004GL019932>.

- Hall, A., 2004. The role of surface albedo feedback in climate. *J. Clim.* 17 (7), 1550–1568. [https://doi.org/10.1175/1520-0442\(2004\)017<1550:TROSAF>2.0.CO;2](https://doi.org/10.1175/1520-0442(2004)017<1550:TROSAF>2.0.CO;2).
- Hansen, J., Nazarenko, L., 2004. Soot climate forcing via snow and ice albedos. *Proc. Natl. Acad. Sci.* 101 (2), 423–428. <https://doi.org/10.1073/pnas.2237157100>.
- Hansen, J., Ruedy, R., Sato, M., Lo, K., 2010. Global surface temperature change. *Rev. Geophys.* 48 (4) <https://doi.org/10.1029/2010RG000345>.
- Hathaway, D.H., 2015. The solar cycle. *Living reviews in solar physics.* 12 (1), 4. <https://doi.org/10.1007/lrsp-2015-4>.
- Haustein, K., Otto, F.E., Venema, V., Jacobs, P., Cowtan, K., Hausfather, Z., Way, R.G., White, B., Subramanian, A., Schurer, A.P., 2019. A limited role for unforced internal variability in twentieth-century warming. *J. Clim.* 32 (16), 4893–4917. <https://doi.org/10.1175/JCLI-D-18-0555.1>.
- Haywood, J., Boucher, O., 2000. Estimates of the direct and indirect radiative forcing due to tropospheric aerosols: a review. *Rev. Geophys.* 38 (4), 513–543. <https://doi.org/10.1029/1999RG000078>.
- Hegerl, G.C., Brönnimann, S., Schurer, A., Cowan, T., 2018. The early 20th century warming: anomalies, causes, and consequences. *Wiley Interdiscip. Rev. Clim. Change* 9 (4), e522. <https://doi.org/10.1002/wcc.522>.
- Iles, C., Hegerl, G., 2017. Role of the North Atlantic Oscillation in decadal temperature trends. *Environ. Res. Lett.* 12, 114010. <https://doi.org/10.1088/1748-9326/aa9152>.
- IPCC, 2001. iii, W.G. Third Assessment Report. Summary for Policymakers - 2001.
- IPCC, 2007. Solomon, S. The Physical Science Basis: Contribution of Working Group I to the fourth assessment report of the Intergovernmental Panel on Climate Change. Intergovernmental Panel on Climate Change (IPCC). Climate Change 2007, p. 996.
- IPCC, 2013. Stocker, T.F., Qin, D., Plattner, G.K., Tignor, M., Allen, S.K., Boschung, J., Nauels, A., Xia, Y., Bex, V. and Midgley, P.M. The Physical Science Basis. Contribution of Working Group I to the Fifth Assessment Report of the Intergovernmental Panel on Climate Change. Intergovernmental Panel on Climate Change (IPCC), Climate change 2013, p. 1535.
- Ivanov, V., Alexeev, V., Koldunov, N.V., Repina, I., Sandø, A.B., Smedsrud, L.H., Smirnov, A., 2016. Arctic Ocean heat impact on regional ice decay: a suggested positive feedback. *J. Phys. Oceanogr.* 46 (5), 1437–1456. <https://doi.org/10.1175/JPO-D-15-0144.1>.
- Ivanov, V., Smirnov, A., Alexeev, V., Koldunov, N.V., Repina, I., Semenov, V., 2018. Contribution of convection-induced heat flux to winter ice decay in the western nansen basin. *J. Geophys. Res. Oceans* 123 (9), 6581–6597. <https://doi.org/10.1029/2018JC013995>.
- Johannessen, O.M., Bengtsson, L., Miles, M.W., Kuzmina, S.I., Semenov, V.A., Alekseev, G.V., Nagurnyi, A.P., Zakharov, V.F., Bobylev, L.P., Pettersson, L.H., Hasselmann, K., 2004. Arctic climate change: observed and modelled temperature and sea-ice variability. *Tellus A* 56 (4), 328–341. <https://doi.org/10.3402/tellusa.v56i4.14418>.
- Kato, S., Rose, F.G., Rutan, D.A., Charlock, T.P., 2008. Cloud effects on the meridional atmospheric energy budget estimated from Clouds and the Earth's Radiant Energy System (CERES) data. *J. Clim.* 21 (17), 4223–4241. <https://doi.org/10.1175/2008JCLI1982.1>.
- Kattsov, V.M., Meleshko, V.P., Govorkova, V.A., 2008. Modeli, prednaznachennye dlia ocenki budushih izmeneniy klimata [Models designed to assess future climate change]. *Trudy GOS. Hydrophis. Observ.* 1 (5), 112–151 (in Russian).
- Kincer, J.B., 1933. Is our climate changing? A study of long-time temperature trends. *Mon. Weather Rev.* 61 (9), 251–259. [https://doi.org/10.1175/1520-0493\(1933\)61<251:IOCCAS>2.0.CO;2](https://doi.org/10.1175/1520-0493(1933)61<251:IOCCAS>2.0.CO;2).
- King, A.D., Black, M.T., Min, S.-K., Fischer, E.M., Mitchell, D.M., Harrington, L.J., Perkins-Kirkpatrick, S.E., 2016. Emergence of heat extremes attributable to anthropogenic influences. *Geophys. Res. Lett.* 43, 3438–3443. <https://doi.org/10.1002/2015GL067448>.
- Koch, D., Hansen, J., 2005. Distant origins of Arctic black carbon: a Goddard Institute for Space Studies ModelE experiment. *J. Geophys. Res. Atmos.* 110 (D4) <https://doi.org/10.1029/2004JD005296>.
- Kosaka, Y., Xie, S.P., 2016. The tropical Pacific as a key pacemaker of the variable rates of global warming. *Nat. Geosci.* 9 (9), 669–673. <https://doi.org/10.1038/ngeo2770>.
- Kravitz, B., Robock, A., 2011. Climate effects of high-latitude volcanic eruptions: role of the time of year. *J. Geophys. Res. Atmos.* 116 (D1) <https://doi.org/10.1029/2010JD014448>.
- Kravtsov, S., Grimm, C., Gu, S., 2018. Global-scale multidecadal variability missing in state-of-the-art climate models. *npj Clim. Atmos. Sci.* 1, 34. <https://doi.org/10.1038/s41612-018-0044-6>.
- Kug, J.S., Jeong, J.H., Jang, Y.S., Kim, B.M., Folland, C.K., Min, S.K., Son, S.W., 2015. Two distinct influences of Arctic warming on cold winters over North America and East Asia. *Nat. Geosci.* 8 (10), 759–762. <https://doi.org/10.1038/ngeo2517>.
- Kuzmina, S.I., Johannessen, O.M., Bengtsson, L., Aniskina, O.G., Bobylev, L.P., 2008. High northern latitude surface air temperature: comparison of existing data and creation of a new gridded data set 1900–2000. *Tellus A* 60 (2), 289–304. <https://doi.org/10.1111/j.1600-0870.2007.00303.x>.
- Laloyaux, P., et al., 2018. CERA-20C: a coupled reanalysis of the twentieth century. *J. Adv. Model. Earth Syst.* 10, 1172–1195. <https://doi.org/10.1029/2018MS001273>.
- Lappo, S.S., Gulev, S.K., Rozhdestvenskii, A.E., 1990. Large-Scale Heat Interaction in the Ocean–Atmosphere System and Energy-Active Zones in the World Ocean. Leningrad, USSR: Gidrometeoizdat (in Russian).
- Latif, M., Böning, C., Willebrand, J., Biastoch, A., Dengg, J., Keenlyside, N., Schweckendiek, U., Madec, G., 2006. Is the thermohaline circulation changing? *J. Clim.* 19 (18), 4631–4637.
- Latif, M., Martin, T., Park, W., 2013. Southern Ocean sector centennial climate variability and recent decadal trends. *J. Clim.* 26 (19), 7767–7782. <https://doi.org/10.1175/JCLI-D-12-00281.1>.
- Latonin, M.M., Bashmachnikov, I.L., Bobylev, L.P., Davy, R., 2021. Multi-model ensemble mean of global climate models fails to reproduce early twentieth century Arctic warming. *Polar Sci.* 100677. <https://doi.org/10.1016/j.polar.2021.100677>.
- Lean, J.L., 2018. Estimating solar irradiance since 850 CE. *Earth Space Sci.* 5 (4), 133–149. <https://doi.org/10.1002/2017EA000357>.
- Lean, J.L., Rind, D.H., 2008. How natural and anthropogenic influences alter global and regional surface temperatures: 1889 to 2006. *Geophys. Res. Lett.* 35 (18) <https://doi.org/10.1029/2008GL034864>.
- Lenssen, N., Schmidt, G., Hansen, J., Menne, M., Persin, A., Ruedy, R., Zyss, D., 2019. Improvements in the GISTEMP uncertainty model. *J. Geophys. Res. Atmos.* 124 (12), 6307–6326. <https://doi.org/10.1029/2018JD029522>.
- Levitus, S., Matishov, G., Seidov, D., Smolyar, I., 2009. Barents Sea multidecadal variability. *Geophys. Res. Lett.* 36 (19) <https://doi.org/10.1029/2009GL039847>.
- Lindsay, R., Wensnahan, M., Schweiger, A., Zhang, J., 2014. Evaluation of seven different atmospheric reanalysis products in the Arctic. *J. Clim.* 27 (7), 2588–2606. <https://doi.org/10.1175/JCLI-D-13-00014.1>.
- Lohmann, U., Feichter, J., 2005. Global indirect aerosol effects: a review. *Atmos. Chem. Phys.* 5 (3), 715–737. <https://doi.org/10.5194/acp-5-715-2005>.
- Luo, D., Xiao, Y., Diao, Y., Dai, A., Franzke, C.L.E., Simmonds, I., 2016. Impact of Ural blocking on winter warm Arctic–cold Eurasian anomalies. Part II: the link to the North Atlantic oscillation. *J. Clim.* 29, 3949–3971. <https://doi.org/10.1175/JCLI-D-15-0612.1>.
- MacFarling Meure, C., Etheridge, D., Trudinger, C., Steele, P., Langenfelds, R., Van Ommen, T., Smith, A., Elkins, J., 2006. Law dome CO₂, CH₄ and N₂O ice core records extended to 2000 years BP. *Geophys. Res. Lett.* 33 (14) <https://doi.org/10.1029/2006GL026152>.
- Malinin, V.N., Vainovsky, P.A., 2018. O prichinah pervogo poteplemiya Arktiki v XX stoletii [On the causes of the first warming of the Arctic in the 20th century]. In: *Scientific Notes of RGGMU*, 53, p. 34 (in Russian).
- Mann, M.E., 2002. Little ice age. *Encycl. Glob. Environ. Change* 1, 504–509.
- Mantua, N.J., Hare, S.R., Zhang, Y., Wallace, J.M., Francis, R.C., 1997. A Pacific interdecadal climate oscillation with impacts on salmon production. *Bull. Am. Meteorol. Soc.* 78 (6), 1069–1080. [https://doi.org/10.1175/1520-0477\(1997\)078<1069:APICOW>2.0.CO;2](https://doi.org/10.1175/1520-0477(1997)078<1069:APICOW>2.0.CO;2).
- Mass, C.F., Portman, D.A., 1989. Major volcanic eruptions and climate: a critical evaluation. *J. Clim.* 2 (6), 566–593. [https://doi.org/10.1175/1520-0442\(1989\)002<0566:MVEACA>2.0.CO;2](https://doi.org/10.1175/1520-0442(1989)002<0566:MVEACA>2.0.CO;2).
- McCabe, G.J., Palecki, M.A., Betancourt, J.L., 2004. Pacific and Atlantic Ocean influences on multidecadal drought frequency in the United States. *Proc. Natl. Acad. Sci.* 101 (12), 4136–4141. <https://doi.org/10.1073/pnas.0306738101>.
- McConnell, J.R., Edwards, R., Kok, G.L., Flanner, M.G., Zender, C.S., Saltzman, E.S., Banta, J.R., Pasteris, D.R., Carter, M.M., Kahl, J.D., 2007. 20th-century industrial black carbon emissions altered arctic climate forcing. *Science* 317 (5843), 1381–1384. <https://doi.org/10.1126/science.1144856>.
- Meehl, G.A., Washington, W.M., Ammann, C.M., Arblaster, J.M., Wigley, T.M.L., Tebaldi, C., 2004. Combinations of natural and anthropogenic forcings in twentieth-century climate. *J. Clim.* 17 (19), 3721–3727. [https://doi.org/10.1175/1520-0442\(2004\)017<3721:CONAAF>2.0.CO;2](https://doi.org/10.1175/1520-0442(2004)017<3721:CONAAF>2.0.CO;2).
- Menon, S., Hansen, J., Nazarenko, L., Luo, Y., 2002. Climate effects of black carbon aerosols in China and India. *Science* 297 (5590), 2250–2253. <https://doi.org/10.1126/science.1075159>.
- Miles, M.W., Divine, D.V., Furevik, T., Jansen, E., Moros, M., Ogilvie, A.E., 2014. A signal of persistent Atlantic multidecadal variability in Arctic sea ice. *Geophys. Res. Lett.* 41 (2), 463–469. <https://doi.org/10.1002/2013GL058084>.
- Miller, R.L., Schmidt, G.A., Nazarenko, L.S., Tausnev, N., Bauer, S.E., DelGenio, A.D., Kelley, M., Lo, K.K., Ruedy, R., Shindell, D.T., Aleinov, I., 2014. CMIP5 historical simulations (1850–2012) with GISS ModelE2. *J. Adv. Model.* 6 (2), 441–478. <https://doi.org/10.1002/2013MS000266>.
- Mokhov, I.I., Semenov, V.A., 2016. Weather and climate anomalies in Russian regions related to global climate change. *Russ. Meteorol. Hydrol.* 41 (2), 84–92. <https://doi.org/10.3103/S1068373916020023>.
- Mokhov, I.I., Smirnov, D.A., 2008. Diagnostics of a cause-effect relation between solar activity and the Earth's global surface temperature. *Atmos. Ocean. Phys.* 44 (3), 263–272. <https://doi.org/10.1134/S0001433808030018>.
- Morice, C.P., Kennedy, J.J., Rayner, N.A., Jones, P.D., 2012. Quantifying uncertainties in global and regional temperature change using an ensemble of observational estimates: The HadCRUT4 data set. *J. Geophys. Res. Atmos.* 17 (D8) <https://doi.org/10.1029/2011JD017187>.
- Morice, C.P., Kennedy, J.J., Rayner, N.A., Winn, J.P., Hogan, E., Killick, R.E., Dunn, R.J. H., Osborn, T.J., Jones, P.D., Simpson, I.R., 2021. An updated assessment of near-surface temperature change from 1850: the HadCRUT5 dataset. *J. Geophys. Res.* 126 (3) <https://doi.org/10.1029/2019JD032361>.
- Moritz, R.E., Bitz, C.M., Steig, E.J., 2002. Dynamics of recent climate change in the Arctic. *Science* 297, 1497–1502. <https://doi.org/10.1126/science.1076522>.
- Najafi, M.R., Zwiers, F.W., Gillett, N.P., 2015. Attribution of Arctic temperature change to greenhouse-gas and aerosol influences. *Nat. Clim. Chang.* 5 (3), 246–249. <https://doi.org/10.1038/nclimate2524>.
- Nozawa, T., Nagashima, T., Shioyama, H., Crooks, S.A., 2005. Detecting natural influence on surface air temperature change in the early twentieth century. *Geophys. Res. Lett.* 32 (20) <https://doi.org/10.1029/2005GL023540>.
- Onarheim, I.H., Eldevik, T., Smedsrud, L.H., Stroeve, J.C., 2018. Seasonal and regional manifestation of Arctic sea ice loss. *J. Clim.* 31 (12), 4917–4932. <https://doi.org/10.1175/JCLI-D-17-0427.1>.

- Otterå, O.H., Bentsen, M., Drange, H., Suo, L., 2010. External forcing as a metronome for Atlantic multidecadal variability. *Nat. Geosci.* 3 (10), 688–694. <https://doi.org/10.1038/ngeo955>.
- Overland, J.E., Dethloff, K., Francis, J.A., Hall, R.J., Hanna, E., Kim, S.J., Screen, J.A., Shepherd, T.G., Vihma, T., 2016. Nonlinear response of mid-latitude weather to the changing Arctic. *Nat. Clim. Chang.* 6 (11), 992–999. <https://doi.org/10.1038/nclimate3121>.
- Owens, M.J., Lockwood, M., Hawkins, E., Usoskin, I., Jones, G.S., Barnard, L., Schurer, A., Fasullo, J., 2017. The Maunder minimum and the Little Ice Age: an update from recent reconstructions and climate simulations. *J. Space Weather Space Clim.* 7, A33. <https://doi.org/10.1051/swsc/2017034>.
- Petoukhov, V., Semenov, V.A., 2010. A link between reduced Barents-Kara sea ice and cold winter extremes over northern continents. *J. Geophys. Res. Atmos.* 115 (D21) <https://doi.org/10.1029/2009JD013568>.
- Philander, S.G., 1990. El Niño, La Niña, and the Southern Oscillation, 293. Academic, San Diego, CA. <https://doi.org/10.1126/science.248.4957.904>.
- Pithan, F., Mauritsen, T., 2014. Arctic amplification dominated by temperature feedbacks in contemporary climate models. *Nat. Geosci.* 7 (3), 181–184. <https://doi.org/10.1038/ngeo2071>.
- Poli, P., Hersbach, H., Dee, D.P., Berrisford, P., Simmons, A.J., Vitart, F., Trémolet, Y., 2016. ERA-20C: an atmospheric reanalysis of the twentieth century. *J. Clim.* 29 (11), 4083–4097. <https://doi.org/10.1175/JCLI-D-15-0556.1>.
- Polyakov, I.V., Bekryaev, R.V., Alekseev, G.V., Bhatt, U.S., Colony, R.L., Johnson, M.A., Maskhtas, A.P., Walsh, D., 2003. Variability and trends of air temperature and pressure in the maritime Arctic, 1875–2000. *J. Clim.* 16 (12), 2067–2077. [https://doi.org/10.1175/1520-0442\(2003\)016<2067:VATOAT>2.0.CO;2](https://doi.org/10.1175/1520-0442(2003)016<2067:VATOAT>2.0.CO;2).
- Polyakov, I.V., Alekseev, G.V., Timokhov, L.A., Bhatt, U.S., Colony, R.L., Simmons, H.L., Walsh, D., Walsh, J.E., Zakharov, V.F., 2004. Variability of the intermediate Atlantic water of the Arctic Ocean over the last 100 years. *J. Clim.* 17 (23), 4485–4497. <https://doi.org/10.1175/JCLI-3224.1>.
- Proshutinsky, A.Y., Johnson, M.A., 1997. Two circulation regimes of the wind-driven Arctic Ocean. *J. Geophys. Res. Oceans* 102 (C6), 12493–12514. <https://doi.org/10.1029/97JC00738>.
- Przybylak, R., Svyashchennikov, P.N., Uscka-Kowalkowska, J., Wyszynski, P., 2020. Solar radiation in the Arctic during the Early Twentieth Century Warming (1921–1950), presenting a compilation of newly available data. *J. Clim.* 1–44. <https://doi.org/10.1175/JCLI-D-20-0257.1>.
- Quaas, J., Boucher, O., Bellouin, N., Kinne, S., 2008. Satellite-based estimate of the direct and indirect aerosol climate forcing. *J. Geophys. Res. Atmos.* 113 (D5) <https://doi.org/10.1029/2007JD008962>.
- Reid, G.C., 1997. Solar forcing of global climate change since the mid-17th century. *Clim. Chang.* 37 (2), 391–405. <https://doi.org/10.1023/A:1005307009726>.
- Robock, A., 2000. Volcanic eruptions and climate. *Rev. Geophys.* 38 (2), 191–219. <https://doi.org/10.1029/1998RG000054>.
- Roe, G., 2009. Feedbacks, timescales, and seeing red. *Ann. Rev. Earth. Planet. Sc.* 37, 93–115. <https://doi.org/10.1146/annurev.earth.061008.134734>.
- Rohde, R., 2013. Comparison of Berkeley Earth, NASA GISS, and Hadley CRU averaging techniques on ideal synthetic data. In: *Berkeley Earth Memo, January, 2, 2013*.
- Rohrer, M., Brönnimann, S., Martius, O., Raible, C.C., Wild, M., Compo, G.P., 2018. Representation of extratropical cyclones, blocking anticyclones, and Alpine circulation types in multiple reanalyses and model simulations. *J. Clim.* 31, 3009–3031. <https://doi.org/10.1175/JCLI-D-17-0350.1>.
- Rypdal, M., Rypdal, K., 2010. Testing hypotheses about sun-climate complexity linking. *Phys. Rev. Lett.* 104 (12) <https://doi.org/10.1103/physrevlett.104.128501>.
- Sato, M., Hansen, J.E., McCormick, M.P., Pollack, J.B., 1993. Stratospheric aerosol optical depths, 1850–1990. *J. Geophys. Res. Atmos.* 98 (D12), 22987–22994. <https://doi.org/10.1029/93JD02553>.
- Scafetta, N., West, B.J., 2008. Is climate sensitive to solar variability? *Phys. Today* 3, 50–51. <https://doi.org/10.1063/1.2897951>.
- Schlesinger, M.E., Ramankutty, N., 1994. An oscillation in the global climate system of period 65–70 years. *Nature* 367 (6465), 723–726. <https://doi.org/10.1038/367723a0>.
- Schlichtholz, P., 2013. Observational evidence for oceanic forcing of atmospheric variability in the Nordic seas area. *J. Clim.* 26 (9), 2957–2975. <https://doi.org/10.1175/JCLI-D-11-00594.1>.
- Schubert, S.D., Suarez, M.J., Pegion, P.J., Koster, R.D., Bacmeister, J.T., 2004. On the cause of the 1930s dust bowl. *Science* 303, 1855–1859.
- Self, S., Rampino, M.R., Barbera, J.J., 1981. The possible effects of large 19th and 20th century volcanic eruptions on zonal and hemispheric surface temperatures. *J. Volcanol. Geotherm. Res.* 11 (1), 41–60. [https://doi.org/10.1016/0377-0273\(81\)90074-3](https://doi.org/10.1016/0377-0273(81)90074-3).
- Semenov, V.A., 2007. Structure of temperature variability in the high latitudes of the Northern Hemisphere. *Atmos. Ocean. Phys.* 43 (6), 687–695. <https://doi.org/10.1134/S0001433807060023>.
- Semenov, V.A., 2008. Influence of oceanic inflow to the Barents Sea on climate variability in the Arctic region. In: *Doklady Earth Sciences*, 418. Springer Nature BV, p. 91. <https://doi.org/10.1007/s11471-008-1020-0>.
- Semenov, V.A., 2015. Modern climate fluctuations caused by feedbacks in the atmosphere–Arctic ice–ocean system. *Fundam. Prikl. Klimatol.* 1 (1), 232–248.
- Semenov, V.A., Bengtsson, L., 2003. Modes of the wintertime Arctic temperature variability. *Geophys. Res. Lett.* 30 (15) <https://doi.org/10.1029/2003GL017112>.
- Semenov, V.A., Latif, M., 2012. The early twentieth century warming and winter Arctic sea ice. *Cryosphere* 6 (6), 1231–1237. <https://doi.org/10.5194/tc-6-1231-2012>.
- Semenov, V.A., Latif, M., 2015. Nonlinear winter atmospheric circulation response to Arctic sea ice concentration anomalies for different periods during 1966–2012. *Geophys. Res. Lett.* 10 (5), 054020 <https://doi.org/10.1088/1748-9326/10/5/054020>.
- Semenov, V.A., Matveeva, T.A., 2020. Arctic sea ice in the first half of the 20th century: temperature-based spatiotemporal reconstruction. *Atmos. Oceanic Phys.* 56 (5), 534–538. <https://doi.org/10.1134/S0001433820050102>.
- Semenov, V.A., Latif, M., Dommenget, D., Keenlyside, N.S., Strehz, A., Martin, T., Park, W., 2010. The impact of North Atlantic–Arctic multidecadal variability on Northern Hemisphere surface air temperature. *J. Clim.* 23 (21), 5668–5677. <https://doi.org/10.1175/2010JCLI3347.1>.
- Semenov, V.A., Shelekhova, E.A., Mokhov, I.I., Zuev, V.V., Koltermann, K.P., 2014. Influence of the Atlantic Multidecadal Oscillation on settling anomalous climate regimes in Northern Eurasia based on model simulation. *Doklady Earth Sci.* 459 (2), 1619. <https://doi.org/10.1134/S1028334X14120307>.
- Serreze, M.C., Francis, J.A., 2006. The Arctic amplification debate. *Clim. Chang.* 76 (3–4), 241–264. <https://doi.org/10.1007/s10584-005-9017-y>.
- Shindell, D., Faluvegi, G., 2009. Climate response to regional radiative forcing during the twentieth century. *Nat. Geosci.* 2 (4), 294–300. <https://doi.org/10.1038/ngeo473>.
- Shiogama, H., Nagashima, T., Yokohata, T., Crooks, S.A., Nozawa, T., 2006. Influence of volcanic activity and changes in solar irradiance on surface air temperatures in the early twentieth century. *Geophys. Res. Lett.* 33 (9) <https://doi.org/10.1029/2005GL025622>.
- Sigurdsson, H., 1990. Evidence of volcanic loading of the atmosphere and climate response. *Palaeogeogr. Palaeoclimatol. Palaeoecol.* 89 (3), 277–289. [https://doi.org/10.1016/0031-0182\(90\)90069-J](https://doi.org/10.1016/0031-0182(90)90069-J).
- Smedsrud, L.H., Esau, I., Ingvaldsen, R.B., Eldevik, T., Haugan, P.M., Li, C., Lien, V.S., Olsen, A., Omar, A.M., Otterå, O.H., Risebrobakken, B., 2013. The role of the Barents Sea in the Arctic climate system. *Rev. Geophys.* 51 (3), 415–449. <https://doi.org/10.1002/rog.20017>.
- Stefan, J., 1879. On the relationship between thermal radiation and temperature. In: *Bulletin From the Sessions of the Vienna Academy of Sciences*, 79, pp. 391–428.
- Steinman, B.A., Mann, M.E., Miller, S.K., 2015. Atlantic and Pacific multidecadal oscillations and Northern Hemisphere temperatures. *Science* 347 (6225), 988–991. <https://doi.org/10.1126/science.1257856>.
- Stephenson, D.B., Wanner, H., Brönnimann, S., Luterbacher, J., 2003. The history of scientific research on the North Atlantic Oscillation. *Geophys. Monogr. Am. Geophys. Union* 134, 37–50. <https://doi.org/10.1029/134GM02>.
- Stolpe, M.B., Medhaug, I., Knutti, R., 2017. Contribution of Atlantic and Pacific multidecadal variability to twentieth-century temperature changes. *J. Clim.* 30 (16), 6279–6295. <https://doi.org/10.1175/JCLI-D-16-0803.1>.
- Stott, P.A., Tett, S.F., Jones, G.S., Allen, M.R., Mitchell, J.F.B., Jenkins, G.J., 2000. External control of 20th century temperature by natural and anthropogenic forcings. *Science* 290 (5499), 2133–2137. <https://doi.org/10.1126/science.290.5499.2133>.
- Suo, L., Otterå, O.H., Bentsen, M., Gao, Y., Johannessen, O.M., 2013. External forcing of the early 20th century Arctic warming. *Tellus A* 65 (1), 20578. <https://doi.org/10.3402/tellusa.v65i0.20578>.
- Svendsen, L., Keenlyside, N., Bethke, I., Gao, Y., Omrani, N.E., 2018. Pacific contribution to the early twentieth-century warming in the Arctic. *Nat. Clim. Chang.* 8 (9), 793–797. <https://doi.org/10.1038/s41558-018-0247-1>.
- Takemura, T., Nozawa, T., Emori, S., Nakajima, T.Y., Nakajima, T., 2005. Simulation of climate response to aerosol direct and indirect effects with aerosol transport-radiation model. *J. Geophys. Res. Atmos.* 110 (D2) <https://doi.org/10.1029/2004JD005029>.
- Tans, P., Keeling, R., 2020. Annual Mean Atmospheric CO₂ Values for Mauna Loa From Pieter Tans, NOAA/ESRL (www.esrl.noaa.gov/gmd/ccgg/trends/) and Dr. Ralph Keeling, Scripps Institution of Oceanography (scrippsco2.ucsd.edu/). available at: <https://www.esrl.noaa.gov/gmd/ccgg/trends/data.html> (last access: 24th April 2020).
- Tett, S.F., Stott, P.A., Allen, M.R., Ingram, W.J., Mitchell, J.F., 1999. Causes of twentieth-century temperature change near the Earth's surface. *Nature* 399 (6736), 569–572. <https://doi.org/10.1038/21164>.
- Titchner, H.A., Rayner, N.A., 2014. The Met Office Hadley Centre sea ice and sea surface temperature data set, version 2: 1. Sea ice concentrations. *J. Geophys. Res. Atmos.* 119 (6), 2864–2889. <https://doi.org/10.1002/2013JD020316>.
- Tokina, H., Xie, S.P., Mukougawa, H., 2017. Early 20th-century Arctic warming intensified by Pacific and Atlantic multidecadal variability. *PNAS* 114 (24), 6227–6232. <https://doi.org/10.1073/pnas.1615880114>.
- Tremblay, L.B., 2001. Can we consider the Arctic Oscillation independently from the Barents Oscillation? *Geophys. Res. Lett.* 28 (22), 4227–4230. <https://doi.org/10.1029/2001GL013740>.
- Twomey, S., 1974. Pollution and the planetary albedo. *Atmos. Environ.* 8 (12), 1251–1256. [https://doi.org/10.1016/0004-6981\(74\)90004-3](https://doi.org/10.1016/0004-6981(74)90004-3).
- Undorf, S., Bollandia, M.A., Hegerl, G.C., 2018. Impacts of the 1900–74 increase in anthropogenic aerosol emissions from North America and Europe on Eurasian summer climate. *J. Clim.* 31 (20), 8381–8399.
- Viebrock, H.J., Flowers, E.C., 1968. Comments on the recent decrease in solar radiation at the South Pole. *Tellus* 20 (3), 400–411. <https://doi.org/10.1111/j.2153-3490.1968.tb00380.x>.
- Vise, V.U., 1937. The reasons of Arctic warming. *Sovetskaya Arktika* 1, 1–7 (in Russian).
- Walsh, J.E., Fetterer, F., Scott Stewart, J., Chapman, W.L., 2017. A database for depicting Arctic sea ice variations back to 1850. *Geogr. Rev.* 107 (1), 89–107. <https://doi.org/10.1111/j.1931-0846.2016.12195.x>.
- Wang, M., Overland, J.E., Kattsov, V., Walsh, J.E., Zhang, X., Pavlova, T., 2007. Intrinsic versus forced variation in coupled climate model simulations over the Arctic during the twentieth century. *J. Clim.* 20 (6), 1093–1107. <https://doi.org/10.1175/JCLI4043.1>.

- Wegmann, M., Brönnimann, S., Compo, G.P., 2017. Tropospheric circulation during the early twentieth century Arctic warming. *Clim. Dyn.* 48 (7–8), 2405–2418. <https://doi.org/10.1007/s00382-016-3212-6>.
- Wegmann, M., Orsolini, Y.J., Zolina, O., 2018. Warm Arctic–cold Siberia: comparing the recent and the early 20th century Arctic warmings. *Environ. Res. Lett.* 13 <https://doi.org/10.1088/1748-9326/aaa0b7>.
- Winton, M., 2006. Amplified Arctic climate change: what does surface albedo feedback have to do with it? *Geophys. Res. Lett.* 33, L03701. <https://doi.org/10.1029/2005GL025244>.
- Wood, K.R., Overland, J.E., 2010. Early 20th century Arctic warming in retrospect. *Int. J. Climatol.* 30 (9), 1269–1279. <https://doi.org/10.1002/joc.1973>.
- Wood, K.R., Overland, J.E., Jónsson, T., Smoliak, B.V., 2010. Air temperature variations on the Atlantic–Arctic boundary since 1802. *Geophys. Res. Lett.* 37, L17708 <https://doi.org/10.1029/2010GL044176>.
- Xu, Y., Ramanathan, V., 2012. Latitudinally asymmetric response of global surface temperature: implications for regional climate change. *Geophys. Res. Lett.* 39 (13) <https://doi.org/10.1029/2012GL052116>.
- Yamanouchi, T., 2011. Early 20th century warming in the Arctic: a review. *Polar Sci.* 5 (1), 53–71. <https://doi.org/10.1016/j.polar.2010.10.002>.
- Zakharov, V.F., 2003. Variations of sea ice area during XX century from historical data. In: Bobylev, L.P., Kondratyev, K.A., Johannessen, O.M. (Eds.), *Arctic Environment Variability in the Context of the Global Change*. Springer-Praxis, pp. 107–236.
- Zhang, R., Delworth, T.L., Sutton, R., Hodson, D.L., Dixon, K.W., Held, I.M., Kushnir, Y., Marshall, J., Ming, Y., Msadek, R., Robson, J., 2013. Have aerosols caused the observed Atlantic multidecadal variability? *Int. J. Atmos. Sci.* 70 (4), 1135–1144. <https://doi.org/10.1175/JAS-D-12-0331.1>.
- Zolotokrylin, A.N., Titkova, T.B., Mikhailov, A.Y., 2014. Climatic variations of the Arctic front and the Barents Sea ice cover in winter time. *Ice Snow* 54 (1), 85–90 in Russian. [10.15356/2076-6734-2014-1-85-90](https://doi.org/10.15356/2076-6734-2014-1-85-90).
- Zorita, E., Von Storch, H., Gonzalez-Rouco, F.J., Cubasch, U., Luterbacher, J., Legutke, S., Fischer-Bruns, I., Schlese, U., 2004. Climate evolution in the last five centuries simulated by an atmosphere-ocean model: global temperatures, the North Atlantic Oscillation and the late Maunder Minimum. *Meteorol. Z.* 13 (4), 271–289. <https://doi.org/10.1127/0941-2948/2004/0013-0271>.